Inorganic Chemistry

Article

pubs.acs.org/IC

End-On and Side-On π-Acid Ligand Adducts of Gold(I): Carbonyl, Cyanide, Isocyanide, and Cyclooctyne Gold(I) Complexes Supported by N-Heterocyclic Carbenes and Phosphines

Mehmet Ali Celik,[†] Chandrakanta Dash,[‡] Venkata A. K. Adiraju,[‡] Animesh Das,[‡] Muhammed Yousufuddin,[‡] Gernot Frenking,*[,†] and H. V. Rasika Dias*[,‡]

[†]Fachbereich Chemie, Philipps-Universität Marburg, D-35039 Marburg, Germany

[‡]Department of Chemistry and Biochemistry, The University of Texas at Arlington, Arlington, Texas 76019-0065, United States

Supporting Information

ABSTRACT: N-Heterocyclic carbene ligand SIDipp (SIDipp = 1,3-bis(2,6-diisopropylphenyl)imidazolin-2-ylidene) and trimesitylphosphine ligand have been used in the synthesis of gold(I) cyanide, *t*-butylisocyanide, and cyclooctyne complexes (SIDipp)Au(CN) (**3**), (Mes_3P)Au(CN) (**4**), [(Mes_3P)$_2$Au][Au(CN)$_2$] (**5**), [(SIDipp)Au(CN^tBu)][SbF_6] ([**6**][$\mathbf{SbF_6}$]), [(SIDipp)Au(cyclooctyne)][SbF_6] ([**8**][$\mathbf{SbF_6}$]), and [(Mes_3P)Au(cyclooctyne)][SbF_6] ([**9**][$\mathbf{SbF_6}$]). A detailed computational study has been carried out on these and the related gold(I) carbonyl adducts [(SIDipp)Au(CO)][SbF_6] ([**1**][$\mathbf{SbF_6}$]), [(Mes_3P)Au(CO)][SbF_6] ([**2**][$\mathbf{SbF_6}$]), and [(Mes_3P)Au(CN^tBu)]$^+$ ([**7**]$^+$). X-ray crystal structures of **3**, **5**, [**6**][$\mathbf{SbF_6}$], [**8**][$\mathbf{SbF_6}$], and [**9**][$\mathbf{SbF_6}$] revealed that they feature linear gold sites. Experimental and computational data show that the changes in π-acid ligand on (SIDipp)Au$^+$ from CO, CN^-, CN^tBu, cyclooctyne as in [**1**]$^+$, **3**, [**6**]$^+$, and [**8**]$^+$ did not lead to large changes in the Au−$C_{carbene}$ bond distances. A similar phenomenon was also observed in Au−P distance in complexes [**2**]$^+$, **4**, [**7**]$^+$, and [**9**]$^+$ bearing trimesitylphosphine. Computational data show that the Au−L bonds of "naked" [Au−L]$^+$ or SIDipp and Mes_3P supported [Au−L]$^+$ (L = CO, CN^-, CN^tBu to cyclooctyne) have higher electrostatic character than covalent character. The Au←L σ-donation and Au→L π-back-donation contribute to the orbital term with the former being the dominant component, but the latter is not negligible. In the Au−CO adducts [**1**]$^+$and [**2**]$^+$, the cationic gold center causes the polarization of the C−O σ and π orbitals toward the carbon end making the coefficients at the two atoms more equal which is mainly responsible for the large blue shift in the CO stretching frequency. The SIDipp and Mes_3P supported gold(I) complexes of cyanide and isocyanide also exhibit a significant blue shift in $\overline{\nu}_{CN}$ compared to that of the free ligands. Calculated results for Au(CO)Cl and Au(CF_3)CO suggest that the experimentally observed blue shift in $\overline{\nu}_{CO}$ of these compounds may at least partly be caused by intermolecular forces.

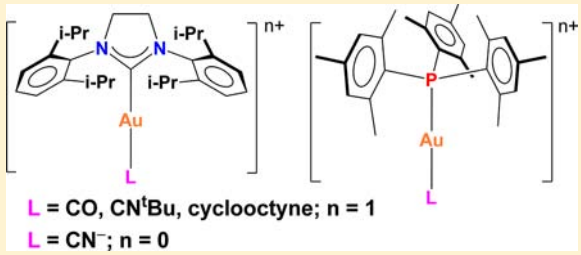

INTRODUCTION

Traditionally, gold is considered as one of the most inert metals and used widely in jewelry industry and in coins. However, recent years have seen the emergence of gold as a facilitator of wide variety of useful reactions especially when used at the atomic level either in pure metal form or as part of a metal complex. In fact, novel reactions mediated by gold are reported in the latest literature in ever-increasing numbers.[1−4] Gold is an excellent choice for various transformations involving carbon monoxide, alkenes, alkynes, allenes, and arenes.[5−8] N-Heterocyclic carbenes or phosphines are used quite often as supporting ligands.[9−15]

An area of research focus in our laboratory concerns the study of molecules featuring bonds between gold(I) and small unsaturated molecules like CO, isocyanide, alkenes, and alkynes.[16−19] Recently we communicated the isolation of gold(I) carbonyl adducts [(SIDipp)Au(CO)][SbF_6] ([**1**][$\mathbf{SbF_6}$]) (SIDipp = 1,3-bis(2,6-diisopropylphenyl)imidazolin-2-ylidene) and [(Mes_3P)Au(CO)][SbF_6] ([**2**][$\mathbf{SbF_6}$]) (Figure 1) using N-heterocyclic carbene and phosphine auxiliary ligands, respectively.[20,21] Such species are of significant interest because they are rare (e.g., structurally characterized species

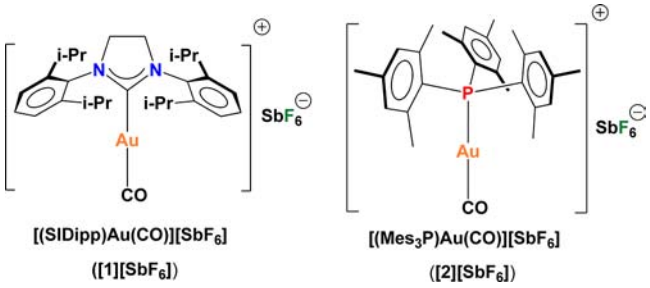

Figure 1. Gold(I) carbonyl complexes supported by N-heterocyclic carbene and phosphine ligands.

Received: August 27, 2012
Published: December 28, 2012

   dx.doi.org/10.1021/ic301869v | *Inorg. Chem.* 2013, 52, 729−742

Table 1. Comparison of Vibrational ($\bar{\nu}_{CO}$, cm^{-1}), Structural (Bond Distances, Å), and NMR Spectroscopic Data (Chemical Shifts, ppm) for Gold(I) Carbonyls

compd	$\bar{\nu}_{CO}$, cm^{-1}	Au−CO, Å	C−O, Å	^{13}CO	ref
CO	2143		1.12822(7)	184 (CD_2Cl_2)	35
$[HB(3,5\text{-}(CF_3)_2Pz)_3]AuCO$	2144	1.862(9)	1.113(11)	173 ($CDCl_3$)	23
Au(CO)Cl	2170	1.93(2)	1.11(3)	172 (CD_2Cl_2)	89,22
Au(CO)Br	2153[a]			174 (CD_2Cl_2)	89
$Au_2(CO)Cl_4$	2180[b]			171 (CD_2Cl_2)	90
$Au(CO)SO_3F$	2196			162 (HSO_3F)	91,92
$[(SIDipp)Au(CO)][SbF_6]$	2197	1.971(5)	1.110 (6)	182.7 (CD_2Cl_2)	20
$[(Mes_3P)Au(CO)][SbF_6]$	2185	2.008(6)	1.108(7)	182.6 (CD_2Cl_2)	21
$Au(CF_3)(CO)$	2194	1.977(16)	1.08(2)	183.0 (CD_2Cl_2)	34
$[Au(CO)][OTeF_5]$	2179				93
$[Au(CO)_2][Sb_2F_{11}]$	2217			174 (HSO_3F)	92
$[Au(CO)_2]_2[SbF_6][Sb_2F_{11}]$	2235.5	1.962(17)	1.153(17)		24
$[Au(CO)_2]_2[SbF_6][Sb_2F_{11}]$	2235.5	1.972(8)	1.107(9)		24
$[Au(CO)_2][UF_6]$	2200				94

[a]In 1,2-dibromoethane. [b]In SO_2Cl_2.

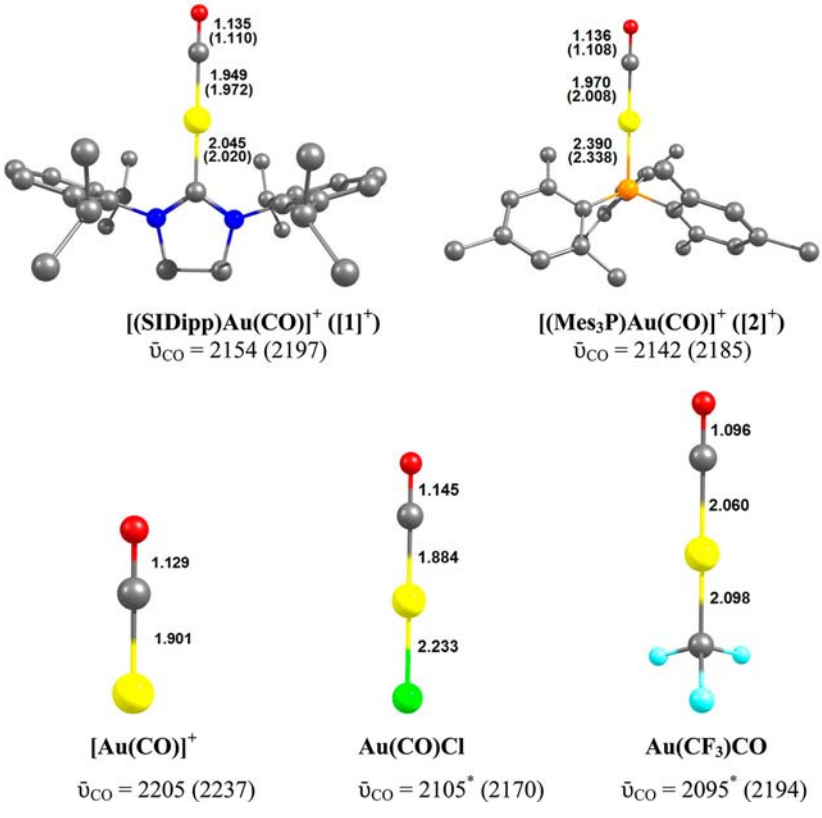

Figure 2. Calculated equilibrium geometries and C−O stretching frequencies of $[(SIDipp)Au(CO)]^+$ ($[\mathbf{1}]^+$), $[(Mes_3P)Au(CO)]^+$ ($[\mathbf{2}]^+$), $[Au(CO)]^+$, Au(CO)Cl, and $Au(CF_3)CO$ at BP86/TZVPP. Bond lengths are given in Å, frequencies in cm^{-1}. Experimental values are given in parentheses. The calculated frequency for free CO is 2126 cm^{-1}. *See the effects of intermolecular forces of Au(CO)Cl and $Au(CF_3)CO$ on $\bar{\nu}_{CO}$ (leading to a blue shift) in the Results and Discussion.

involving terminal Au−CO bonds were limited to Au(CO)Cl,[22] $[HB(3,5\text{-}(CF_3)_2Pz)_3]Au(CO)$,[23] and $[Au(CO)_2]_2[SbF_6][Sb_2F_{11}]$[24] until recently), serve as useful models for likely intermediates in relevant gold catalyzed processes involving carbon monoxide,[7,25−27] and provide valuable spectroscopic and structural data.

In this Article, we report additional details on these compounds as well as the synthesis of gold(I) complexes featuring cyanide and isocyanide. The main focus of this study is to examine the structures, bonding, and properties of closely related end-on bound π-acceptor ligand (CO, CN^-, CN^tBu) adducts of gold(I) having the same supporting ligand. We picked N-heterocyclic carbene SIDipp (SIDipp = 1,3-bis(2,6-diisopropylphenyl)imidazolin-2-ylidene) as one of the supporting ligands for this purpose as it represents an increasingly important group of ligands in gold chemistry. We also synthesized a second series of compounds using Mes_3P (instead of SIDipp), which represents yet another group of important auxiliary ligands in gold chemistry. The two categories allow us to investigate the influence of the

dx.doi.org/10.1021/ic301869v | Inorg. Chem. 2013, 52, 729−742

supporting ligand. Furthermore, synthesis and structural data on two new gold(I) alkyne complexes (an area of high topical interest)[5,17,28−31] are also included in this study. They provide information on gold(I) adducts involving side-on bound π-acid ligands.

RESULTS AND DISCUSSION

In 2011, we communicated that it is possible to use N-heterocyclic carbenes and phosphines to isolate cationic gold(I) carbonyl adducts like [(SIDipp)Au(CO)][SbF_6] and [(Mes_3P)Au(CO)][SbF_6].[20,21] Key structural and spectroscopic parameters of these and several other isolable or spectroscopically observed gold(I) adducts are summarized in Table 1. Interestingly, [(SIDipp)Au(CO)][SbF_6] and [(Mes_3P)Au(CO)][SbF_6] have rather high CO stretching frequencies which are higher than in free CO (2143 cm^{-1}). Since most metal carbonyls have C−O modes which are less than 2143 cm^{-1}, the former class has been termed by Strauss "nonclassical carbonyls".[32,33] A quantum chemical investigation was carried out in order to understand the unusual frequency shift of the C−O stretching mode toward higher wave numbers. The Au(CO)Cl and Au(CF_3)CO (reported by Fornies and co-workers)[34] were also included in this study for comparison because they are neutral molecules but display the same feature.

Figure 2 shows the calculated geometries and C−O stretching frequencies of the cations [(SIDipp)Au(CO)]$^+$ ([**1**]$^+$), [(Mes_3P)Au(CO)]$^+$ ([**2**]$^+$), and [Au(CO)]$^+$ and the neutral gold carbonyls Au(CO)Cl and Au(CF_3)CO. The agreement between the calculated and experimental bond lengths in [**1**]$^+$ and [**2**]$^+$ is quite good. The theoretical values for the CO stretching mode are always somewhat smaller than the experimental data and so is the calculated frequency for free CO (2126 cm^{-1}) compared with experiment (2143 cm^{-1}).[35] Nevertheless, calculations give a blue shift toward higher wave numbers for [**1**]$^+$ and [**2**]$^+$ which agrees with experimental findings. The largest value for a CO stretching mode is calculated for [Au(CO)]$^+$ (2205 cm^{-1}) which also agrees with the experimental observations that "naked" [Au(CO)]$^+$ (2237 cm^{-1})[36] and salt compounds of [Au(CO)]$^+$ with various counterions exhibit significant blue shifts (Table 1).

Interestingly, for Au(CO)Cl and Au(CF_3)CO, a small red-shift is calculated which is not what was observed experimentally. We note however that Au(CO)Cl and Au(CF_3)CO adducts have intermolecular Au···Au interactions in the solid state.[22,34,37,38] It is also known that the CO stretch value of Au(CO)Cl in solution depends on the solvent. Therefore, in order to find out whether intermolecular forces might induce a blue shift for the CO stretching mode of these molecules, we investigated the $\bar{\nu}_{CO}$ values of small aggregates. The pentamer of Au(CO)Cl having constrained C_{4v} symmetry was chosen as a model for this study. Indeed, frequency calculations of [Au(CO)Cl]$_5$ show that the central Au(CO)Cl species which is surrounded by four neighboring molecules (see Supporting Information) has a higher CO stretching mode of 2146 cm^{-1} which gives a blue shift of 20 cm^{-1} (relative to the calculated frequency for free CO of 2126 cm^{-1}). In the case of Au(CF_3)CO we found that already a dimer exhibits a higher CO stretching frequency of 2132 cm^{-1} yielding a blue shift of 6 cm^{-1}. It means that the experimentally observed blue shifts of Au(CO)Cl and Au(CF_3)CO and perhaps other carbonyls may at least partly be caused by intermolecular interactions.

Table 2 gives the results of the EDA-NOCV calculations. It is interesting to note that the Au−CO interactions in the cation [Au(CO)]$^+$ are only slightly stronger (ΔE_{int} = −58.9 kcal/mol) than in neutral ClAuCO (ΔE_{int} = −55.6 kcal/mol). Since the preparation energies of the fragments are very small, the absolute values of the interaction energies are nearly the same as the bond dissociation energies (BDEs) which are D_e = 58.8 kcal/mol for [Au(CO)]$^+$ and D_e = 55.5 kcal/mol for Au(CO)Cl. The latter values are probably about 12 kcal/mol too high. Previous high-level ab initio studies gave D_e = 45.1 kcal/mol at the QCISD(T) level for [Au(CO)]$^+$ and D_e = 43.5 kcal/mol at CCSD(T) for ClAuCO.[39,40] The trend of the Au−CO bond strength in the five molecules can be expected to be correct. Systematic studies of transition metal carbonyls have shown that standard DFT methods faithfully reproduce trends of bond dissociation energies which are calculated by highly accurate ab initio methods such as CCSD(T).[41]

Table 2. EDA-NOCV Results at BP86/TZ2P+//BP86/TZVPP for the Au−CO Bonds of [(SIDipp)Au(CO)]$^+$ ([1**]$^+$), [(Mes_3P)Au(CO)]$^+$ ([**2**]$^+$), [Au(CO)]$^+$, Au(CO)Cl, and Au(CF_3)CO with Energy Values in kcal/mol**

fragments	(SIDipp) Au^+ + CO	(Mes_3P) Au^+ + CO	Au^+ + CO	ClAu + CO	(CF_3)Au + CO
ΔE_{int}	−44.3	−33.4	−58.9	−55.6	−36.5
ΔE_{pauli}	151.0	168.3	201.3	189.5	163.8
ΔE_{elstat}[a]	−122.9 (63.0%)	−127.4 (63.1%)	−159.7 (61.4%)	−153.8 (62.8%)	−126.9 (63.3%)
ΔE_{orb}[a]	−72.3 (37.1%)	−74.3 (36.9%)	−100.5 (38.6%)	−91.2 (37.2%)	−73.5 (36.5%)
ΔE_{σ}[b]	−41.8 (57.8%)	−44.9 (61.4%)	−66.7 (66.4%)	−46.5 (51.0%)	−40.9 (55.7%)
ΔE_{π}[b]	−29.0 (40.2%)	−28.2 (38.0%)	−32.2 (32.0%)	−43.2 (47.4%)	−31.0 (42.2%)
ΔE_{rest}[b]	−1.5 (2.0%)	−1.2 (0.6%)	−1.1 (1.6%)	−1.5 (1.6%)	−1.6 (2.2%)
ΔE_{prep}	1.2	1.2	0.1	0.1	3.8
D_e	43.1	32.2	58.8	55.5	32.7

[a]The values in parentheses are the percentage contributions to the total attractive interactions ΔE_{elsat} + $\Delta E_{orbital}$. [b]The values in parentheses are the percentage contributions to the total orbital interactions $\Delta E_{orbital}$.

Table 2 shows that the Au−CO bonds in the five molecules have a rather uniformly higher electrostatic character than covalent character. The Coulombic attraction ΔE_{elstat} which comes mainly from the overlap of the σ lone-pair electrons of CO with the nucleus of Au[42] contributes between 61% and 63% to the total attraction while the orbital interactions ΔE_{orb} contribute only between 37% and 39%. It is at first sight surprising that the orbital term comprises a rather larger contribution from π orbitals. Table 2 shows that ΔE_{π} contributes between 32.0% and 47.4% to ΔE_{orb}. Nonclassical carbonyls which exhibit a blue shift of the CO stretching frequency are considered to possess only negligible metal→CO π-backdonation.[32,33,43−45] We want to point out that ΔE_{orb} not only comes from genuine orbital interactions, it also comes from the polarization of the orbitals within the fragments. The large contributions of ΔE_{π} in the gold carbonyl complexes arise from the significant polarization of the occupied π orbitals in CO and in the metal fragments. The polarization of the occupied π and σ orbitals of CO toward the carbon end which is induced by the positive charge of the metal fragments is the main reason for the observed blue shift of the CO stretching frequencies.[33]

Cyanide ion is isoelectronic to carbon monoxide. It is however considered as a better σ-donor and a relatively poor π-

dx.doi.org/10.1021/ic301869v | Inorg. Chem. 2013, 52, 729−742

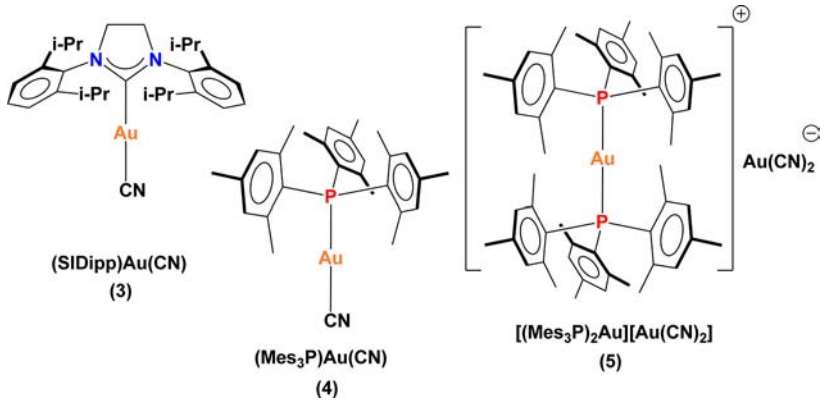

Figure 3. Gold(I) cyanide complexes supported by N-heterocyclic carbene and phosphine ligands and the disproportionated product of $(Mes_3P)Au(CN)$.

Table 3. Comparison of Vibrational ($\bar{\upsilon}_{CN}$, cm^{-1}), Structural (Bond Distances, Å), and NMR Spectroscopic Data (Chemical Shifts, ppm) for Gold(I) Cyanides (TPA = 1,3,5-Triaza-7-phosphaadamantane, I^{t}Bu = 1,3-Di-*t*-butylimidazol-2-ylidene, IDipp =1,3-Bis(2,6-diisopropylphenyl)imidazol-2-ylidene)

compd	$\bar{\upsilon}_{CN}$ cm^{-1}	Au−CN, Å	C−N, Å	Au−P or Au−C_{carb}, Å	^{13}CN	ref
$Et_4N(CN)$	2050					95
$(Et_3P)Au(CN)$	2138	1.97(2)	1.15(3)	2.288(5)	158.2($CDCl_3$)	50
$(Cy_3P)Au(CN)$		2.006(11)	1.128(13)	2.287(3)		96
$(Ph_3P)Au(CN)$	2147	2.003(7)	1.136(10)	2.278(2)		49
$\{Ph_2(Cy)P\}Au(CN)$		2.073(13)	1.04(2)	2.284(3)		97
$\{(m\text{-tolyl})_3P\}Au(CN)$		2.087(10)	1.02(2)	2.286(3)		96,97
$[(TPA)_2Au][Au(CN)_2]$	2143	2.02(3)	1.16(4)	2.302(5)		54
$[\{(CNCH_2CH_2)_3P\}_2Au][Au(CN)_2]$		1.77(4)	1.13(5)	2.314(5)		98
$[\{(CNCH_2CH_2)_3P\}_2Au][Au(CN)_2]$		2.22(3)	0.98(3)	2.322(5)		98
$[(Mes_3P)_2Au][Au(CN)_2]$	2142	1.979(10)	1.124(13)	2.3275(19)[a]	151.5($CDCl_3$)	this work
$[(Mes_3P)_2Au][Au(CN)_2]$	2142	2.000(10)	1.114(12)	2.3311(19)[a]	151.5($CDCl_3$)	this work
$(I^tBu)Au(CN)$	2148	2.009(7)	1.098(10)	2.011(6)	150.1($CDCl_3$)	46
(IDipp)Au(CN)		1.996(17)	1.117(19)	1.985(15)	152.3($CDCl_3$)	47
(SIDipp)Au(CN)	2151	2.058(5)	1.099(7)	2.039(5)	152.4($CDCl_3$)	this work

[a]From the two half molecules in unit cell.

acceptor ligand. N-Heterocyclic carbene and phosphine adducts of gold(I) cyanide, (SIDipp)Au(CN) (**3**) and $(Mes_3P)Au(CN)$ (**4**) (see Figure 3), are neutral molecules and are useful systems for structure and bonding comparisons with corresponding gold carbonyls. The gold(I) cyanide complex (SIDipp)Au(CN) was synthesized in good yield by the reaction of (SIDipp)AuCl with KCN. It is an air stable, colorless compound and has been characterized by NMR, IR spectroscopy, elemental analysis, and X-ray crystallography. The corresponding ^{13}C labeled adduct was also synthesized via a similar route using K^{13}CN (instead of KCN). The $^{13}C\{^1H\}$ NMR spectrum of (SIDipp)Au(^{13}CN) in $CDCl_3$ showed a doublet ($^2J_{CC}$ = 41.9 Hz) at δ 206.9 ppm which can be assigned to the gold bound N-heterocyclic carbene carbon resonance. The ^{13}C resonance of the cyanide carbon appeared at δ 152.4 ppm which is in a region comparable to other reported N-heterocyclic carbene gold(I) cyanide complexes such as [(1,3-di-*t*-butylimidazol-2-ylidene)-Au(CN)] (150.1 ppm)[46] and [(1,3-*bis*(2,6-diisopropylphenyl)-imidazol-2-ylidene)Au(CN)] (152.3 ppm)[47] (Table 3). IR spectrum of (SIDipp)Au(CN) showed a strong signal corresponding to the CN stretch at 2151 cm^{-1}.

The X-ray crystal structure of (SIDipp)Au(CN) (**3**) is depicted in Figure 4. It crystallizes in the *Pbcm* space group and featured a linear geometry at the gold(I) with C1−Au−C15 angle of 178.62(19)°. The bond lengths of Au−C1 and Au−CN are 2.039(5) and 2.058(5) Å, respectively. It is possible to compare the *trans* influence of CN^- ligand to their isoelectronic CO ligand. Interestingly, the Au−C1 distance in (SIDipp)Au-(CN) [2.039(5) Å] is not that different from the corresponding

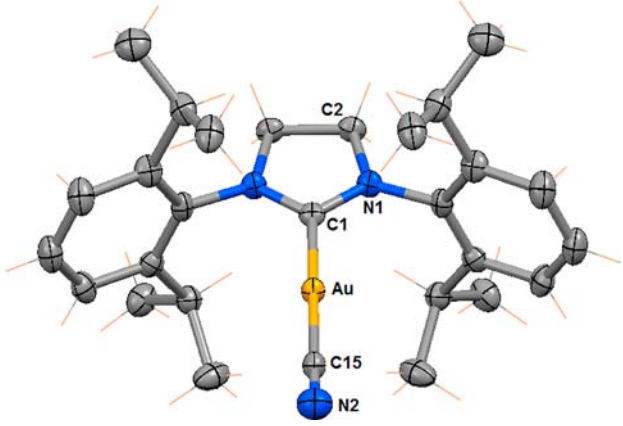

Figure 4. Molecular structure showing (SIDipp)Au(CN) (**3**), ellipsoids are shown at 50% probability level. Selected bond lengths (Å) and angles (deg): Au−C1 2.039(5), Au−C15 2.058(5), N2−C15 1.099(7), C1−Au−C15 178.62(19), N2−C15−Au 177.6(5), N1−C1−N1 109.7(4).

dx.doi.org/10.1021/ic301869v | *Inorg. Chem.* 2013, 52, 729−742

Au−C distance of the [(SIDipp)Au(CO)][SbF_6] [2.020(4) Å]. However, the Au−C1 bond distance in the gold(I) chloride adduct (SIDipp)AuCl is marginally shorter [1.979(3) Å].[48]

The synthesis of gold(I) cyanide complex (Mes_3P)Au(CN) (**4**) was attempted by the reaction of (Mes_3P)AuCl with KCN. The corresponding ^{13}C labeled adduct (^{13}**4**) was also synthesized via a similar route using $K^{13}CN$ (instead of KCN). However, unlike (SIDipp)Au(CN), the trimesitylphosphine supported Au^ICN complex was isolated as an ionic species, [(Mes_3P)$_2$Au][Au(CN)$_2$] (**5**), in the solid state. This is not always the case for phosphine supported Au^ICN adducts as other neutral complexes such as $Ph_3PAu(CN)$ and $Et_3PAu(CN)$ are known in the solid state (Table 3).[49,50] The ionic species presumably formed due to the ligand scrambling in the solution. The presence of two species, (Mes_3P)Au(^{13}CN) (^{13}**4**) and [(Mes_3P)$_2$Au][Au(^{13}CN)$_2$] (^{13}**5**), in $CDCl_3$ solution at room temperature was confirmed by $^{31}P\{^1H\}$ NMR and $^{13}C\{^1H\}$ NMR spectroscopy. The phosphorus signal for ^{13}**4** was observed as a doublet at δ 5.32 ppm ($^2J_{C,P}$ = 121 Hz) whereas ^{13}**5** displays a broad singlet at δ 6.33 ppm, which is very similar to the other reported [(Mes_3P)$_2$Au][BF_4] complex (δ 6.3 ppm).[51] The $^{13}C\{^1H\}$ resonance of the anion in ^{13}**5** appears at δ 151.5 ppm, while in ^{13}**4** it appeared as a doublet ($^2J_{C,P}$ = 121 Hz) at δ 150.4 ppm. For comparison, the $^{13}C\{^1H\}$ NMR of (Et_3P)Au(^{13}CN) in $CDCl_3$ solution displays a resonance at δ 148.6 ppm for [(Et_3P)$_2$Au][Au(^{13}CN)$_2$] and a doublet at δ 158.2 ppm ($^2J_{C,P}$ = 122.4 Hz) for (Et_3P)Au(^{13}CN).[50,52]

[(Mes_3P)$_2$Au][Au(CN)$_2$] (**5**) (grown from dichloromethane by slow evaporation at room temperature) crystallizes in the $P2_1/n$ space group, and the gold atom of the cationic moiety [(Mes_3P)$_2$Au]$^+$ adopts a linear geometry with a P−Au−P angle of 180.0° and an inversion center at Au. The cation and the anion in **5** are well separated (Figure 5), and the shortest distance between two gold atoms is about 10.96 Å. The average Au−P distance of 2.3293(19) Å in **5** is similar to the corresponding distance found in the [(Mes_3P)Au(CO)][SbF_6] [2.3380(12) Å][21] and [(Mes_3P)$_2$Au][BF_4] [2.3525(10)].[53] The average Au−C distance of 1.989(10) Å in **5** is similar to the Au−C bond length found in [(1,3,5-triaza-7-phosphaadamantane)$_2$Au][Au(CN)$_2$] (2.02(3) Å).[54] These two compounds have the same [Au(CN)$_2$]$^-$ anion.

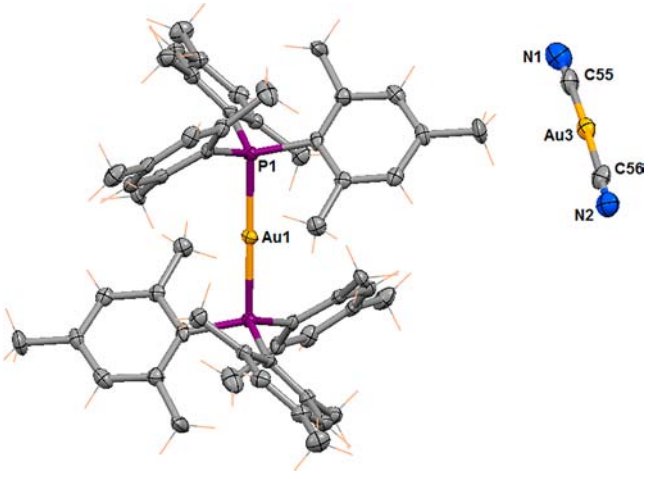

Figure 5. Molecular structure showing [(Mes_3P)$_2$Au][Au(CN)$_2$] (**5**), ellipsoids are shown at 50% probability level. Only one of the two [(Mes_3P)$_2$Au]$^+$ moieties present in the asymmetric unit is shown. Selected bond lengths (Å) and angles (deg): Au1−P1 2.3275(19), Au2−P2 2.3311(19), Au3−C55 1.979(10), Au3−C56 2.000(10), N1−C55 1.124(13), N2−C56 1.114(12); P1−Au1−P1 180.0, P2−Au2−P2 180.0, C55−Au3−C56 178.5(4), N1−C55−Au3 177.0(9), N2−C56−Au3 177.7(9).

Figure 6 shows the calculated equilibrium geometries of [(SIDipp)Au(CN)] (**3**), [(Mes_3P)Au(CN)] (**4**), [(Mes_3P)$_2$Au]$^+$, [Au(CN)$_2$]$^-$, and AuCN. The theoretical and experimental values for the bond lengths are in reasonable agreement. The calculated C−N stretching frequencies are very close to the experimental values. A comparison with the calculated value for the stretching mode of free CN^- (2061 cm^{-1}) shows that all the complexes exhibit a significant blue shift of ∼100 cm^{-1}. We also calculated the reaction energy for the disproportionation of **3** and **4**:

$$2[(SIDipp)Au(CN)](\mathbf{3}) \rightarrow [(SIDipp)_2Au]^+ + [Au(CN)_2]^- + 62.9\ \text{kcal/mol} \quad (1)$$

$$2[(Mes_3P)Au(CN)](\mathbf{4}) \rightarrow [(Mes_3P)_2Au]^+ + [Au(CN)_2]^-(\mathbf{5}) + 50.0\ \text{kcal/mol} \quad (2)$$

The calculations suggest that the disproportionation reactions of **3** and **4** yielding ionic species are intrinsically disfavored, which should be expected. However, the charged compounds which are formed will be stabilized by the solvent. Assuming that the stabilization of the ions which are formed in the disproportionation reaction has a similar strength, the disproportionation of **4** is more likely than that of **3** because reaction 2 is less endergonic than reaction 1. This is in agreement with experimental observation that compounds **5** along with **4** are present as a mixture in solution while there is no sign of the forward reaction 1.

Table 4 gives the results of the EDA-NOCV calculations for [(SIDipp)Au(CN)], [(Mes_3P)Au(CN)], [Au(CN)$_2$]$^-$, and Au(CN). The [Au]$^+$/CN^- interactions of [(SIDipp)Au(CN)], [(Mes_3P)Au(CN)], and Au(CN) are significantly stronger than for the carbonyl complexes (Table 2), because the cyanide complexes feature bonding of charged species. The bonding comes mainly from the interactions between the carbon σ lone-pair electrons and Au via electrostatic attraction and through [Au]←CN^- σ-donation which contributes the largest part (<70%) to the total orbital interactions ΔE_{orb}. The π orbital interactions in the cyano complexes are much weaker than in the carbonyl complexes. This is reasonable because CN^- is a much weaker π-acceptor than CO.[55−57] The contribution of ΔE_π to the total binding comes mainly from the polarization of the π orbital rather than genuine [Au]→CN^- π-backdonation.

Isocyanide adducts are also related closely to the corresponding metal cyanide and carbonyl complexes. Thus, gold(I) isocyanide complex [(SIDipp)Au(CN^tBu)][SbF_6] ([**6**][**SbF_6**]) was also synthesized for a comparison of structure, bonding, and properties. It was obtained from the reaction between (SIDipp)AuCl and ^{t}BuNC in the presence of $AgSbF_6$ and characterized by several spectroscopic techniques and X-ray crystallography. It is a colorless crystalline solid and can be stored for several weeks in nitrogen atmosphere at room temperature without any decomposition. IR spectrum of [**6**][**SbF_6**] displays a strong band at 2244 cm^{-1} which can be assigned to the CN stretch. The increase in $\overline{\upsilon}_{CN}$ upon coordination to gold(I) is normal as evident from CN stretch of the Au(CN^tBu) adducts like [HB(3,5-(CF_3)$_2$Pz)$_3$]Au-

dx.doi.org/10.1021/ic301869v | Inorg. Chem. 2013, 52, 729−742

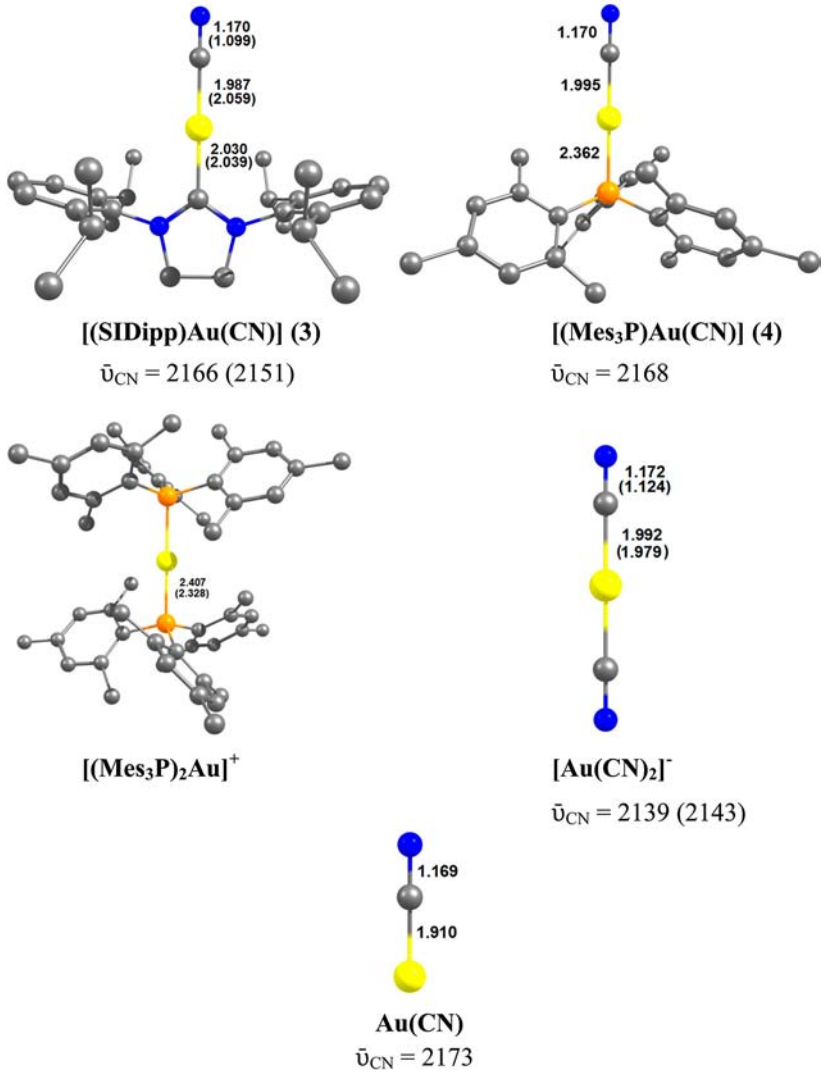

Figure 6. Calculated equilibrium geometries and C−N stretching frequencies of [(SIDipp)Au(CN)] (**3**), [(Mes_3P)Au(CN)] (**4**), [(Mes_3P)$_2$Au]$^+$, [Au(CN)$_2$]$^-$, and Au(CN) at BP86/TZVPP. Bond lengths are given in Å, frequencies in cm^{-1}. Experimental values are given in parentheses. The calculated frequency for free CN$^-$ is 2061 cm^{-1}.

(CN^tBu) [2248 cm^{-1}] and (*p*-$TolSO_2S$)Au(CN^tBu) [2238 cm^{-1}] (Table 5). For comparison, the free *t*-butylisocyanide ligand shows ν_{CN} stretch at 2135 cm^{-1}. The protons of *t*-Bu group in [**6**][**SbF$_6$**] appeared as a singlet at 1.47 ppm in the ^{1}H NMR spectrum which is not much different from the chemical shift value observed for the corresponding protons of the free ligand at 1.42 ppm.

The gold(I) isocyanide complex [(SIDipp)Au(CN^tBu)]-[SbF_6] ([**6**][**SbF$_6$**]) crystallizes in the $P\bar{1}$ space group with two chemically similar molecules in the asymmetric unit (Figure 7). The geometry at the gold is essentially linear with C−Au−C angle of about 178°. The average Au−$C_{carbene}$ distance in [**6**][**SbF$_6$**] is 2.018(4) Å which is similar to the corresponding distance in gold(I) cyanide complex [(SIDipp)-Au(CN)] (**3**) [2.039(5) Å].

The synthesis of phosphine supported gold(I) isocyanide complex, [(Mes_3P)Au(CN^tBu)][SbF_6], was attempted by the reaction of ClAu(CN^tBu) with Mes_3P in the presence of $AgSbF_6$. The analysis of the resulting crystalline product using X-ray crystallography indicated the formation of [(Mes_3P)$_2$Au]-[SbF_6] as one of the products, pointing to a likely ligand redistribution in solution during the synthesis. We did not pursue the isolation of [(Mes_3P)Au(CN^tBu)][SbF_6] any further.

Figure 8 shows the calculated geometries of [(SIDipp)Au-(CN^tBu)]$^+$ ([**6**]$^+$), [(Mes_3P)Au(CN^tBu)]$^+$ ([**7**]$^+$), [Au-(CN^tBu)]$^+$, and Au(CN^tBu)Cl. The EDA results are given in Table 6. The agreement between the calculated and experimental bond lengths in [**6**]$^+$ is quite good. The calculated frequency for the CN stretching mode in the [(SIDipp)Au-(CN^tBu)]$^+$ ([**6**]$^+$) (2227 cm^{-1}) shows a significant blue shift compared to the calculated value for the free ligand CN^tBu (2127 cm^{-1}). This is in excellent agreement with the experimental observations. [(Mes_3P)Au(CN^tBu)]$^+$ ([**7**]$^+$) adducts also predicted a blue shift (although bit smaller compared to the related (SIDipp) supported system). As with the Au−CO systems, "naked" [Au(CN^tBu)]$^+$ shows the highest calculated CN frequency. It is also interesting to note that the Au(CN^tBu)Cl has a calculated $\overline{\nu}_{CN}$ value of 2194 cm^{-1}, which is a blue shift relative to that of the free CN^tBu even without considering any intermolecular interactions.

It is also interesting to compare the experimental and calculated $\overline{\nu}_{CN}$ values of ClAu(CN^tBu) and [(SIDipp)Au-(CN^tBu)][SbF_6]. Experimentally, neutral ClAu(CN^tBu) shows

dx.doi.org/10.1021/ic301869v | *Inorg. Chem.* 2013, 52, 729−742

Table 4. EDA-NOCV Results at BP86/TZ2P+//BP86/TZVPP for the Au−CN Bonds of [(SIDipp)Au(CN)] (3), [(Mes_3P)Au(CN)] (4), $[Au(CN)_2]^-$, and AuCN with Energy Values in kcal/mol

fragments	(SIDipp)Au^+ + CN^-	(Mes_3P)Au^+ + CN^-	(NC)Au + CN^-	Au^+ + CN^-
ΔE_{int}	−164.0	−155.1	−106.1	−230.4
ΔE_{pauli}	187.3	202.9	182.4	261.4
ΔE_{elstat}[a]	−266.5 (75.9%)	−262.4 (73.3%)	−214.9 (74.5%)	−371.33 (75.5%)
ΔE_{orb}[a]	−84.8 (24.1%)	−95.6 (26.7%)	−73.5 (25.5%)	−120.5 (24.5%)
ΔE_{σ}[b]	−59.4 (70.0%)	−71.5 (74.8%)	−54.5 (74.1%)	−90.1 (74.8%)
ΔE_{π}[b]	−13.7 (16.2%)	−13.4 (14.0%)	−16.5 (22.4%)	−23.8 (19.8%)
ΔE_{rest}[b]	−11.7 (13.8%)	−10.7 (11.2%)	−2.5 (3.5%)	−6.6 (5.4%)
ΔE_{prep}	2.3	1.7	0.2	0.2
D_e	161.7	153.4	105.9	230.2

[a]The values in parentheses are the percentage contributions to the total attractive interactions ΔE_{elsat} + $\Delta E_{orbital}$. [b]The values in parentheses are the percentage contributions to the total orbital interactions $\Delta E_{orbital}$.

a much larger shift in the $\overline{\nu}_{CN}$ compared to the cationic [(SIDipp)Au(CN^tBu)][SbF_6] upon CN^tBu coordination (for example, the $\overline{\nu}_{CN}$ of [(SIDipp)Au(CN^tBu)][SbF_6] (2244 cm^{-1}) is more closer to the free CN^tBu (2135 cm^{-1}) than ClAu(CN^tBu) (2260 cm^{-1})). However, calculations indicate a much larger shift in the $\overline{\nu}_{CN}$ for the cationic [(SIDipp)Au(CN^tBu)]$^+$ ([**6**]$^+$) compared to the neutral Au(CN^tBu)Cl upon CN^tBu coordination (for comparison, computed values for the three species are 2227, 2194, and 2127 cm^{-1}, respectively). We think that the difference between the calculated and experimental frequency shift trends may come from intermolecular interactions which we did not include in calculations and should be particularly large (and also experimentally observed) for the Au(CN^tBu)Cl.[38] As we computed for Au(CO)Cl and Au(CF_3)CO, such interactions could induce an additional blue shift in $\overline{\nu}_{CN}$ for Au(CN^tBu)Cl.

Table 6 gives the results of the EDA-NOCV calculations for the isocyanide adducts. A comparison to the analogous carbonyl adducts (Table 2) indicates that the [Au]−CN^tBu interactions are stronger (Table 2) perhaps because CN^tBu is a much better σ-donor than the CO. The bonding comes mainly from the interactions between the carbon σ lone-pair electrons and Au via electrostatic attraction and through [Au]←CN^tBu σ-donation which is similar to that noted above for the corresponding CO adducts. Both these contributions however are slightly larger in the CN^tBu adducts. The π orbital interaction in the CN^tBu complexes is somewhat weaker than in the carbonyl complexes but stronger compared to the cyanide analogues (Table 4).

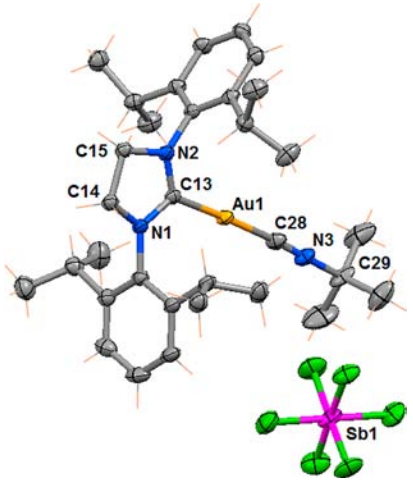

Figure 7. Molecular structure showing [(SIDipp)Au(CN^tBu)][SbF_6] ([**6**][SbF_6]) ellipsoids shown at 50% probability level. Only one of the molecules (out of two) present in the asymmetric unit is shown. Selected bond lengths (Å) and angles (deg): Au1−C13 2.022(4), Au2−C45 2.015(4), Au1−C28 1.988(4), Au2−C60 1.983(4), C28−N3 1.142(5), C60−N6 1.146(5), C29−N3 1.473(5), C61−N6 1.463(5), C14−C15 1.528(5), C46−C47 1.530(6), C28−Au1−C13 177.62(15), C60−Au2−C45 177.65(16), N1−C13−N2 109.9(3), N4−C45−N5 108.8(3), C28−N3−C29 179.3(5), C60−N6−C61 177.2(4), N3−C28−Au1 176.3(4), N6−C60−Au2 177.5(4).

We have also examined the chemistry of gold cyclooctyne adducts supported by phosphines and N-heterocyclic carbenes. Isolable gold(I) alkyne complexes are still fewer in number and are of interest as models for intermediates in gold mediated processes involving alkynes.[17,18,58−63] Keep in mind however that in contrast to the π-acid ligands like CO, CN^-, and CN^tBu which use a lone pair of electrons on carbon to coordinate to metals in end-on fashion, alkynes use π-electrons and bind to metals in side-on fashion.

Cationic gold(I) π-alkyne complexes, [(SIDipp)Au(cyclooctyne)][SbF_6] ([**8**][SbF_6]) and [(Mes_3P)Au(cyclooctyne)][SbF_6] ([**9**][SbF_6]), were synthesized and

Table 5. Comparison of Vibrational ($\overline{\nu}_{CN}$, cm^{-1}), Structural (bond distances, Å), and NMR Spectroscopic Data (chemical shifts, ppm) for Gold(I) Isocyanides

compound	$\overline{\nu}_{CN}$ cm^{-1}	Au−CN, Å	C−N, Å	Au−C_{carb}, Å	ref
CN^tBu	2135				99
ClAu(CN^tBu)	2260	1.92(1)	1.13(2)		100,101
BrAu(CN^tBu)	2235.8	1.939(8)	1.13(1)		102
NCAu(CN^tBu)	2224	1.93(3)	1.21(3)		103
(NO_3)Au(CN^tBu)	2258	1.92(1)	1.13(2)		104
(*p*-$TolSO_2S$)Au(CN^tBu)	2238	1.972(4)	1.135(6)		105
[Au(C≡$CSiMe_3$)(CN^tBu)]	2230	1.98(5)	1.17(5)		106
[HB(3,5-$(CF_3)_2Pz)_3$]Au(CN^tBu)	2248	1.939(8)	1.131(10)		23
[(IMes)Au{CN(2,6-$Me_2C_6H_3$)}][BF_4]	2218.8	1.954(6)	1.171(7)	1.998(5)	107
[(SIDipp)Au(CN^tBu)][SbF_6]	2244	1.986(4)[a]	1.144(5)[a]	2.018(4)[a]	this work

[a]Average distances.

dx.doi.org/10.1021/ic301869v | *Inorg. Chem.* 2013, 52, 729−742

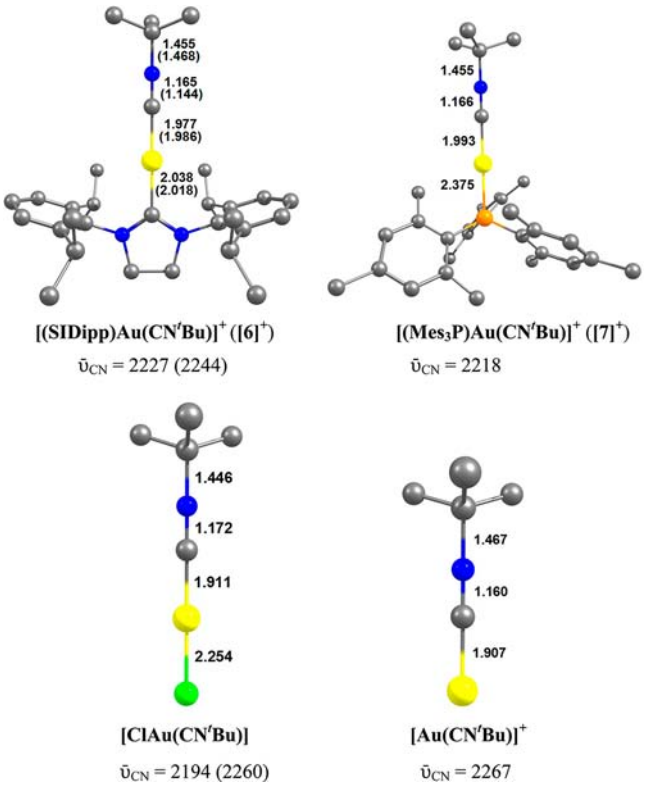

Figure 8. Calculated equilibrium geometries of [(SIDipp)Au(CN^{t}Bu)]$^+$ ([**6**]$^+$), [(Mes$_3$P)Au(CN^{t}Bu)]$^+$ ([**7**]$^+$), [ClAu(CN^{t}Bu)], and [Au(CN^{t}Bu)]$^+$ at BP86/TZVPP. Bond lengths are given in Å. Experimental values are given in parentheses. The calculated CN stretching frequency for free CN^{t}Bu is 2127 cm^{-1}.

Table 6. EDA-NOCV Results at BP86/TZ2P+//BP86/TZVPP for the Au-CN^{t}Bu Bonds [(SIDipp)Au(CN^{t}Bu)]$^+$ ([6]$^+$), [(Mes$_3$P)Au(CN^{t}Bu)]$^+$ ([7]$^+$), [ClAu(CN^{t}Bu)], and [Au(CN^{t}Bu)]$^+$ with Energy Values in kcal/mol

fragments	(SIDipp)Au$^+$ + CN^{t}Bu	(Mes$_3$P)Au$^+$ + CN^{t}Bu	ClAu + CN^{t}Bu	Au$^+$ + CN^{t}Bu
ΔE_{int}	−66.0	−54.7	−65.2	−101.1
ΔE_{pauli}	159.4	176.2	197.7	223.2
ΔE_{elstat} [a]	−156.7 (69.5%)	−158.2 (68.5%)	−182.9 (69.6%)	−216.8 (66.9%)
$\Delta E_{orbital}$ [a]	−68.7 (30.5%)	−72.7 (31.5%)	−80.0 (30.4%)	−107.5 (33.2%)
ΔE_{σ} [b]	−44.5 (64.7%)	−50.2 (69.1%)	−47.8 (59.7%)	−72.9 (67.8%)
ΔE_{π} [b]	−21.3 (31.0%)	−20.4 (28.1%)	−30.6 (38.2%)	−30.8 (28.6%)
ΔE_{rest} [b]	−2.9 (4.2%)	−2.1 (2.9%)	−1.6 (2.0%)	−3.8 (3.5%)
ΔE_{prep}	1.7	1.8	0.1	0.8
D_e	64.3	52.9	65.1	100.3

[a]The values in parentheses are the percentage contributions to the total attractive interactions ΔE_{elsat} + $\Delta E_{orbital}$. [b]The values in parentheses are the percentage contributions to the total orbital interactions $\Delta E_{orbital}$.

isolated from the reaction of the corresponding LAuCl (L = SIDipp and Mes$_3$P) salts, cyclooctyne, and AgSbF$_6$ in dichloromethane at 0 °C in good yield (Figure 9). These gold(I) π-alkyne complexes are thermally stable white solids and have been characterized by NMR, elemental analysis, and X-ray crystallography.

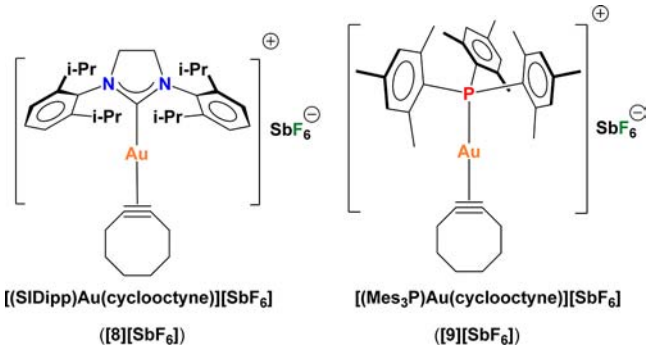

Figure 9. Gold(I) cyclooctyne complexes supported by N-heterocyclic carbene and phosphine ligands.

The [(SIDipp)Au(cyclooctyne)][SbF$_6$] ([**8**][**SbF$_6$**]) is stable in CD_2Cl_2 solution even at room temperature, whereas [(Mes$_3$P)Au(cyclooctyne)][SbF$_6$] ([**9**][**SbF$_6$**]) decomposes slowly in CD_2Cl_2 solution forming black deposits. In this regard it is worth noting that the gold(I) alkyne complex [{(3,5-(CF$_3$)$_2$C$_6$H$_3$)$_3$P)}Au(2-hexyne)][BF$_4$] also quickly decomposes at higher temperature (>223 K) yielding [{(3,5-(CF$_3$)$_2$C$_6$H$_3$)$_3$P)}$_2$Au][BF$_4$] and colloidal gold.[62] The cyclooctyne coordination to the gold(I) in solution was confirmed from the ^{13}C NMR spectrum. In the ^{13}C{^{1}H} NMR spectrum of the gold(I) π-alkyne complex [**8**][**SbF$_6$**] displayed a resonance at δ 97.4 ppm corresponding to the C≡C carbon signal of cyclooctyne, which shows downfield field shift relative to that of the free cyclooctyne C≡C carbon chemical shift value (δ 94.9 ppm).[58] It is interesting to note that the strong σ-donor properties of carbene ligand resulted in the upfield shift of C≡C carbon signal in [**8**][**SbF$_6$**] complex (δ 97.4 ppm) compared to the related phosphine adducts [**9**][**SbF$_6$**] (δ 101.9 ppm). The protons on the α-carbons of the alkyne moiety in [**8**][**SbF$_6$**] also exhibit a larger upfield shift (δ 2.02 ppm) in comparison to the corresponding phosphine analogue (δ 2.66 ppm). The corresponding ^{1}H NMR resonance signal in the free cyclooctyne appears at δ 2.13 ppm. The ^{31}P{^{1}H} NMR spectrum of [(Mes$_3$P)Au(cyclooctyne)][SbF$_6$] exhibited a resonance at δ 6.39 ppm which is a downfield shift compared to that of the [(Mes$_3$P)Au(CO)][SbF$_6$] (δ −4.7) and free Mes$_3$P signal (δ −35.9).

The X-ray quality crystals of the complex [(SIDipp)Au(cyclooctyne)][SbF$_6$] ([**8**][**SbF$_6$**]) were grown from the slow diffusion of hexanes into a CH_2Cl_2 solution at −5 °C. The molecular structure of [**8**][**SbF$_6$**] is depicted in Figure 10. As expected, the gold center adopts a linear geometry with the C(carbene)−Au−cyclooctyne(centroid) angle of 178.13°. The Au−C3 and Au−(C≡C centroid) distances are 2.022(3) and 2.115 Å, respectively. Interestingly, the imidazole plane is nearly perpendicular to the C29−Au−C28 plane with a dihedral angle of ca. 88.15°. The Au−(C≡C centroid) distance of [**8**][**SbF$_6$**] [2.115 Å] is marginally shorter than the corresponding parameter of N-heterocyclic carbene analogue [(IDipp)Au(cyclododecyne)][SbF$_6$] [2.142(5) Å] reported by Fürstner.[63] The C≡C bond distance in complex [**8**][**SbF$_6$**] [1.213(5) Å] is similar to that reported cationic gold complex, [(cyclooctyne)$_3$Au][SbF$_6$] [1.213(7)−1.217(7) Å].[58] There are no close Au···Au or Au···F contacts in the [**8**][**SbF$_6$**] complex.

The molecular structure of [(Mes$_3$P)Au(cyclooctyne)][SbF$_6$] ([**9**][**SbF$_6$**]) is shown in Figure 11. It crystallizes in the $P\bar{1}$ space group. There are two molecules of [(Mes$_3$P)Au-

dx.doi.org/10.1021/ic301869v | Inorg. Chem. 2013, 52, 729−742

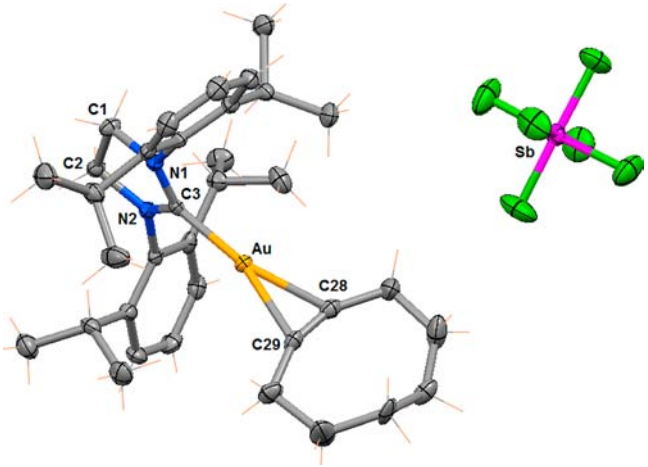

Figure 10. Molecular structure showing [(SIDipp)Au(cyclooctyne)]-[SbF_6] ([**8**][**SbF_6**]), ellipsoids are shown at 50% probability level. Selected bond lengths (Å) and angles (deg): Au−C3 2.022(3), Au−C28 2.199(3), Au−C29 2.201(4), C28−C29, 1.213(5), C1−C2 1.512(5), C3−Au−C28 163.05(13), C3−Au−C29, 164.78(13), C28−C29−C30 157.0(4), C29−C28−C35 157.5(4), C28−Au−C29 32.00(13), N1−C3−N2 108.8(3).

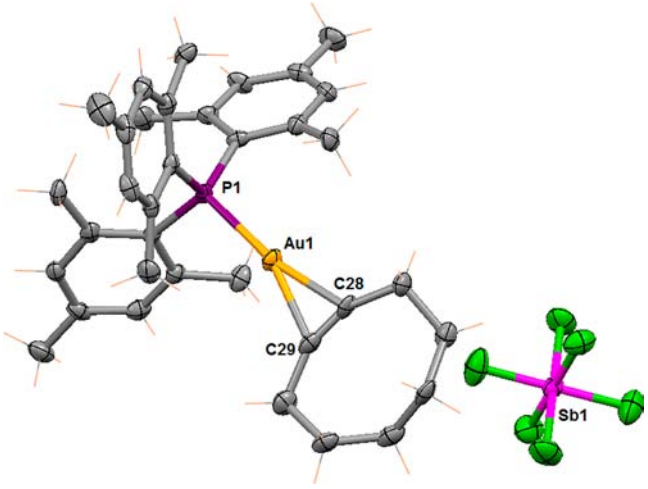

Figure 11. Molecular structure showing [(Mes_3P)Au(cyclooctyne)]-[SbF_6] ([**9**][**SbF_6**]), ellipsoids are shown at 50% probability level. Only one of the molecules (out of two) present in the asymmetric unit is shown. Selected bond lengths (Å) and angles (deg): Au1−P1 2.3220(15), Au2−P2 2.3087(14), Au1−C28 2.223(6), Au2−C63 2.191(5), Au1−C29 2.197(6), Au2−C64 2.188(6), P1−C1 1.843(6), P1−C10 1.850(6), P1−C19 1.841(6), P2−C36 1.835(6), P2−C45 1.836(6), P2−C54 1.831(6), C28−C29 1.223(9), C63−C64 1.203(9), P1−Au1−C28 160.20(17), P1−Au1−C29 166.73(17), P2−Au2−C63 168.43(18), P2−Au2−C64 159.51(19), C28−C29−C30 154.3(7), C29−C28−C35 158.8(7), C63−C64−C65 157.0(6), C64−C63−C70 156.7(6), C29−Au1−C28 32.1(2), C64−Au2−C63 31.9(2).

(cyclooctyne)][SbF_6] in the asymmetric unit. The structure showed a slightly distorted linear conformation with (C≡C centroid)−Au−P angles of 174.75° and 175.25° for the two molecules. The average Mes_3P−Au bond length in [**9**][**SbF_6**] is 2.3153(15) Å, and it is longer than the Au−P distance of (Mes_3P)AuCl (2.2634(15) Å).[64] The average C≡C bond distance of [**9**][**SbF_6**] [1.213(9) Å] is identical to the corresponding distances in N-heterocyclic carbene analogue [**8**][**SbF_6**] [1.213(5) Å] and [(cyclooctyne)$_3$Au][SbF_6] [1.213(7)−1.217(7) Å].

Figure 12 shows the calculated geometries of [(SIDipp)Au-(cyclooctyne)]$^+$ ([**8**]$^+$), [(Mes_3P)Au(cyclooctyne)]$^+$ ([**9**]$^+$),

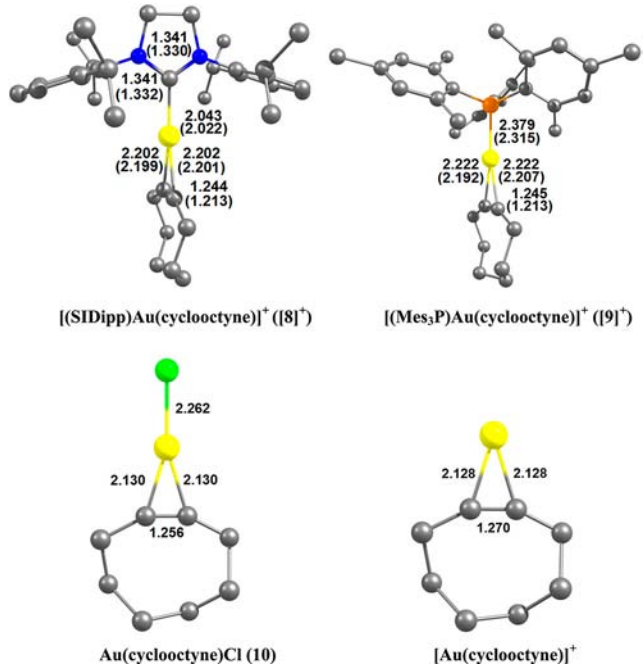

Figure 12. Calculated equilibrium geometries of [(SIDipp)Au-(cyclooctyne)]$^+$ ([**8**]$^+$), [(Mes_3P)Au(cyclooctyne)]$^+$ ([**9**]$^+$), [ClAu-(cyclooctyne)] (**10**), and [Au(cyclooctyne)]$^+$ at BP86/TZVPP. Bond lengths are given in Å. Experimental values are given in parentheses. The calculated C≡C stretching frequency for free cyclooctyne is 2259 cm^{-1}.

[Au(cyclooctyne)]$^+$, and Au(cyclooctyne)Cl (**10**). The EDA results are given in Table 7. The calculated bond lengths of [**8**]$^+$ and [**9**]$^+$ show a very good agreement with the experimental data (Figure 12). The intrinsic interaction energy between the gold fragment and cyclooctyne is significantly higher in [Au(cyclooctyne)]$^+$ (ΔE_{int} = −100.7 kcal/mol) compared to [**8**]$^+$, [**9**]$^+$, and **10**, pointing to notable supporting ligand effect. The electrostatic interaction (ΔE_{elstat}) predominates over the orbital interactions (ΔE_{orb}) in [**8**]$^+$, [**9**]$^+$, [Au(cyclooctyne)]$^+$, and **10**. The breakdown of ΔE_{orb} into contributions of orbitals that have different symmetry shows that the ([C≡C]→Au) σ-donation is the larger component in these adducts and it is the significantly larger component based on percentage contributions to the total orbital interactions $\Delta E_{orbital}$ in the cationic adducts [**8**]$^+$, [**9**]$^+$, and [Au(cyclooctyne)]$^+$, while in the neutral adduct **10**, the σ-contribution is relatively lower and the −C≡C−→Au backbonding is much higher.

Overall, SIDipp and Mes_3P supported gold(I) complexes of carbonyl, cyanide, isocyanide, and cyclooctyne reported in this paper are monomeric, two-coordinate species and display linear geometry at gold(I). The gold(I) carbonyl adducts [(SIDipp)-Au(CO)][SbF_6] ([**1**][**SbF_6**]) and [(Mes_3P)Au(CO)][SbF_6] ([**2**][**SbF_6**]) are air sensitive and thermally less stable compared to the related gold(I) cyanide, isocyanide, and cyclooctyne complexes. The gold(I) cyanides are air stable, whereas the solid samples of gold(I) isocyanide and cyclooctyne adducts are moderately air stable but best stored under an inert atmosphere at −10 °C refrigerator. The stability of gold(I) cyanides is also supported from the computational data. The SIDipp and Mes_3P supported Au−CN bond strength is much stronger (D_e =

dx.doi.org/10.1021/ic301869v | Inorg. Chem. 2013, 52, 729−742

Table 7. EDA-NOCV results at BP86/TZ2P+//BP86/TZVPP for the Au-cyclooctyne bonds [(SIDipp)Au(cyclooctyne)]$^+$ ([8]$^+$), [(Mes_3P)Au(cyclooctyne)]$^+$ ([9]$^+$), [ClAu(cyclooctyne)] and [Au(cyclooctyne)]$^+$ with Energy values in kcal/mol

fragments	(SIDipp)Au$^+$ + cyclooctyne	(Mes_3P)Au$^+$ + cyclooctyne	ClAu + cyclooctyne	Au$^+$ + cyclooctyne
ΔE_{int}	−54.2	−44.8	−57.0	−100.7
ΔE_{pauli}	133.2	148.2	169.6	178.8
ΔE_{elstat} [a]	−117.51 (62.7%)	−121.4 (62.9%)	−144.6 (63.8%)	−162.7 (58.2%)
$\Delta E_{orbital}$ [a]	−69.9 (37.3%)	−71.5 (37.1%)	−82.0 (36.2%)	−116.8 (41.8%)
ΔE_{σ} [b] (−C≡C−→Au)	−34.2 (48.9%)	−36.8 (51.5%)	−38.4 (46.8%)	−68.8 (58.9%)
$\Delta E_{\pi\parallel}$ [b] (Au→−C≡C−)	−20.7 (29.6%)	−20.0 (28.0%)	−33.8 (41.2%)	−28.0 (24.0%)
$\Delta E_{\pi\perp}$ [b] (−C≡C−→Au)	−3.7 (5.2%)	−3.9 (5.5%)	−3.0 (3.7%)	−11.4 (9.8%)
ΔE_{rest}	−11.3 (16.2%)	−10.8 (15.1%)	−6.8 (8.3%)	−8.6 (7.4%)
ΔE_{prep}	3.2	3.4	3.2	4.6
D_e	51.0	41.4	53.8	96.1
$\bar{\upsilon}_{CC}$ [cm^{-1}]	2099.6	2093.7	2040.9	1982.3
r(C≡C) [Å]	1.244	1.245	1.256	1.270

[a]The values in parentheses are the percentage contributions to the total attractive interactions $\Delta E_{elsat} + \Delta E_{orbital}$. [b]The values in parentheses are the percentage contributions to the total orbital interactions $\Delta E_{orbital}$.

161.7, 153.4 kcal/mol) than the gold(I) interaction with CO (D_e = 43.1, 32.2 kcal/mol), CN^{t}Bu (D_e = 64.3, 52.9 kcal/mol), and cyclooctyne (D_e = 51.0, 41.4 kcal/mol) supported by the same auxiliary ligands. The Au−L (CO, CN$^-$, CN^{t}Bu, cyclooctyne) bonds are relatively stronger in the SIDipp systems compared to the corresponding Mes_3P adducts. Interestingly, D_e values of cationic Au(I)CO, CN^{t}Bu, and cyclooctyne systems show that end-on bound Au−CO bonds are the weakest while the corresponding Au−isocyanide contacts are the strongest. The side-on bound Au−cyclooctynes show intermediate bond strengths among the three types. The "naked" [Au(CO)]$^+$, [Au(CN^{t}Bu)]$^+$, and [Au(cyclooctyne)]$^+$ systems have much stronger Au−ligand bonds compared to the corresponding SIDipp and Mes_3P supported systems.

Experimental and computational data show that the changes in unsaturated ligand on (SIDipp)Au$^+$ from CO, CN$^-$, CN^{t}Bu to cyclooctyne as in [**1**]$^+$, **3**, [**6**]$^+$, and [**8**]$^+$ did not lead to notable changes in the Au−$C_{carbene}$ bond distances. A similar phenomenon was also observed in Au−P distance in complexes [**2**]$^+$, **4**, [**7**]$^+$, and [**9**]$^+$ bearing trimesitylphosphine ligands. In solution $^{13}C\{^1H\}$ NMR spectra, the gold(I) bonded carbene carbon resonance of the complexes [**1**][SbF_6] (195.4 ppm), **3** (206.9 ppm), [**6**][SbF_6] (199.9 ppm), and [**9**][SbF_6] (202.5 ppm) was observed in somewhat narrow region of 195−207 ppm. This shows that different types of ligands like CN$^-$, CN^{t}Bu, and cyclooctyne did not have much effect on gold-bound carbene carbon shift.

Calculated frequencies for the CO and CN stretching modes of SIDipp and Mes_3P supported gold(I) adducts of carbonyl, cyanide, and isocyanide reported here show a blue shift compared to the corresponding stretch of the free ligands. These data agree with the experimental results. In the case of neutral gold(I) carbonyls Au(CO)Cl and Au(CF_3)CO, small red shifts were predicted for CO stretching modes of monomers but they changed to blue shifts upon inclusion of intermolecular interactions.

We did not analyze the gold(I)−carbene and Au(I)−phosphine bond strengths of the present complexes. However, relative stabilities suggest that the SIDipp ligand binds to gold(I) much stronger than the Mes_3P. There are computational studies on other molecules supporting this trend.[65]

In summary, we present here structures, properties, and computational data on closely related end-on bound π-acceptor ligand (CO, CN$^-$, CN^{t}Bu) adducts of gold(I) and side-on bound cyclooctyne on gold(I) having the same supporting ligand. We are presently investigating the related chemistry of lighter members of coinage metal family.

EXPERIMENTAL SECTIONS

General Procedures. All manipulations were carried out under an atmosphere of dry nitrogen, using standard Schlenk techniques or in a glovebox. Solvents were purchased from commercial sources, purified using an Innovative Technology SPS-400 PureSolv solvent drying system degassed by the freeze−pump−thaw method twice prior to use. Glassware was oven-dried at 150 °C overnight. NMR spectra were recorded at 298 K on JEOL Eclipse 500 and 300 spectrometer. Proton and carbon chemical shifts are reported in ppm, and referenced using the residual proton and carbon signals of the deuterated solvent. ^{31}P NMR chemical shifts were referenced to a 85% H_3PO_4 standard. The ^{31}P NMR spectroscopic data were accumulated with ^1H decoupling. NMR annotations used are as follows: br = broad, d = doublet, m = multiplet, s = singlet, t = triplet, sept = septet. Infrared spectra were recorded on a JASCO FT-IR 410 spectrometer operating at 2 cm^{-1} spectral resolution. IR spectroscopic data were collected using KBr pellets or mulls between NaCl plates prepared using solid material and Nujol. Herein we use abbreviations based on IUPAC guidelines, that is, υ for frequency and $\bar{\upsilon}$ for wavenumber. Elemental analyses were performed using a Perkin-Elmer Series II CHNS/O analyzer. Cyclooctyne,[66] and (SIDipp)AuCl[48] and (Mes_3P)AuCl[67] were synthesized using literature procedure. Mes_3P, ^{t}BuNC, KCN, K^{13}CN, AuCl, and $AgSbF_6$ were purchased from Sigma-Aldrich and used without further purification.

*[(SIDipp)Au(CN)] (**3**).* A mixture of (SIDipp)AuCl (0.073 g, 0.117 mmol) and KCN (0.008 g, 0.117 mmol) in ethanol (ca. 30 mL) was stirred overnight at room temperature (for (SIDipp)Au(^{13}CN) the K^{13}CN was used). The solvent was removed under reduced pressure. The residue was dissolved in dichloromethane (ca. 20 mL) and filtered, and the filtrate was concentrated to ∼2 mL under reduced pressure. The solution was kept in a refrigerator at 0 °C to obtain colorless prism shaped crystals of (SIDipp)Au(CN) (0.056 g, 78% yield). ^1H NMR ($CDCl_3$, 500.16 MHz, 298 K): δ 7.42 (t, 2H, $^3J_{HH}$ = 8 Hz, C_6H_3), 7.23 (d, 4H, $^3J_{HH}$ = 8 Hz, C_6H_3), 4.05 (s, 4H, CH_2), 3.00 (sept, 4H, $^3J_{HH}$ = 6.9 Hz, $CH(CH_3)_2$), 1.37 (d, 12H, $^3J_{HH}$ = 6.9 Hz, $CH(CH_3)_2$), 1.33 (d, 12H, $^3J_{HH}$ = 6.9 Hz, $CH(CH_3)_2$). $^{13}C\{^1H\}$ NMR ($CDCl_3$, 125.77 MHz, 298 K): δ 206.9 (d, $^2J_{CC}$ = 41.9 Hz, Au−N^{13}CN), 152.4 (^{13}CN), 146.6, 133.6, 130.3, 124.8, 53.9, 29.1, 25.3, 24.2. IR (KBr, selected bands) cm^{-1}: 2151 (CN). IR (Nujol mull, selected bands) cm^{-1}: 2151 (CN). Anal. Calcd for $C_{28}H_{38}N_3Au{\cdot}CH_2Cl_2$: C, 49.86; H, 5.77; N, 6.02. Found: C, 49.70; H, 5.50; N, 5.82%.

*[(Mes_3P)$_2$Au][Au(CN)$_2$] (**5**).* A mixture of Mes_3P (0.167 g, 0.430 mmol) and AuCl (0.099 g, 0.430 mmol) in dichloromethane (ca. 10

dx.doi.org/10.1021/ic301869v | Inorg. Chem. 2013, 52, 729−742

Table 8. Crystallographic Data

	[(SIDipp)Au(CN)]	[$(Mes_3P)_2Au$][$Au(CN)_2$]	[(SIDipp)Au(CN^tBu)][SbF_6]	[(SIDipp)Au(cyclooctyne)][SbF_6]	[(Mes_3P)Au(cyclooctyne)][SbF_6]
formula	$C_{28}H_{38}N_3Au{\cdot}CH_2Cl_2$	$C_{56}H_{66}N_2P_2Au_2{\cdot}2CH_2Cl_2$	$C_{32}H_{47}F_6N_3SbAu{\cdot}2CH_2Cl_2$	$C_{35}H_{50}F_6N_2SbAu{\cdot}CH_2Cl_2$	$C_{35}H_{45}F_6PSbAu{\cdot}0.5CH_2Cl_2$
fw	698.51	1392.83	1076.32	1016.41	971.86
T (K)	100(2)	100(2)	100(2)	100(2)	100(2)
cryst syst	orthorhombic	monoclinic	triclinic	monoclinic	triclinic
space group	$Pbcm$	$P2_1/n$	$P\bar{1}$	$P2_1/c$	$P\bar{1}$
cell dimensions	a = 8.150(8) Å	a = 12.1018(9) Å	a = 12.410(4) Å	a = 14.1827(9) Å	a = 11.8942(13) Å
	b = 16.321(17) Å	b = 28.890(2) Å	b = 14.622(4) Å	b = 14.4496(9) Å	b = 15.9993(18) Å
	c = 23.29(2) Å	c = 16.0447(12) Å	c = 23.418(7) Å	c = 22.4045(11) Å	c = 19.680(2) Å
	α = 90°	α = 90°	α = 82.180(4)°	α = 90°	α = 79.001(1)°
	β = 90°	β = 90.694(1)°	β = 82.853(3)°	β = 120.917(3)°	β = 86.028(1)°
	γ = 90°	γ = 90°	γ = 85.706(4)°	γ = 90°	γ = 77.996(1)°
V (Å)^3	3098(6)	5609.2(7)	4170(2)	3939.1(4)	3594.1(7)
Z	4	4	4	4	4
d_{calcd} (g cm^{-3})	1.498	1.649	1.714	1.714	1.796
abs coeff (mm^{-1})	4.942	5.511	4.472	4.597	5.003
F (000)	1392	2752	2112	2000	1900
θ range (deg)	1.75−28.19	1.41−28.34	1.41−28.47	1.67−28.30	1.32−28.34
reflns collected	22 602	54 830	41 541	38 446	35 171
R_{int} (indep reflns)	0.0521 (3860)	0.0574 (13986)	0.0230 (20698)	0.0369 (9780)	0.0392 (17638)
data/restr/params	3860/0/183	13 986/6/634	20 698/6/905	9780/0/460	17 638/60/894
GOF on F^2	1.103	1.222	1.052	1.062	1.036
R1 [$I > 2\sigma(I)$]/all data	0.0306/0.0365	0.0596/0.0757	0.0353/0.0423	0.0333/0.0424	0.0506/0.0705
wR2 [$I > 2\sigma(I)$]/all data	0.0735/0.0761	0.1300/0.1351	0.0919/0.0965	0.0808/0.0849	0.1283/0.1393

mL) stirred for 2 h at room temperature. The solution was filtered through a pad of Celite via canula, and the filtrate was evaporated to dryness. The residue was dissolved in ethanol (ca. 15 mL), and KCN (0.028 g, 0.430 mmol) was added (for the preparation of [$(Mes_3P)_2Au$][$Au(^{13}CN)_2$] the $K^{13}CN$ was used). The reaction mixture was stirred for overnight at room temperature. The solvent was removed under reduced pressure, the residue was dissolved dichloromethane (ca. 10 mL) and filtered, and the solvent was removed under reduced pressure to give the product as a white solid. Single crystals for X-ray analysis were obtained by slow evaporation from dichloromethane solution. ^{31}P NMR ($CDCl_3$, 121.66 MHz, 298 K) [$(Mes_3P)_2Au$][$Au(CN)_2$]: δ 6.35 (br s). [(Mes_3P)Au(CN)]: δ 5.32 (s). IR (KBr, selected bands) cm^{-1}: 2142 (CN). Anal. Calcd for $C_{56}H_{66}N_2P_2Au_2$: C, 55.00; H, 5.44; N, 2.29. Found: C, 56.00; H, 5.41; N, 2.00%.

[$(Mes_3P)_2Au$][$Au(^{13}CN)_2$] (0.107 g, 41% Yield). $^{13}C\{^1H\}$ NMR ($CDCl_3$, 125.77 MHz, 298 K, selected peaks) [$(Mes_3P)_2Au$][$Au(^{13}CN)_2$]: δ 151.5 (Au−^{13}CN). [(Mes_3P)Au(^{13}CN)]: δ 150.4 (d, $^2J_{C,P}$ = 121 Hz, Au−^{13}CN). $^{31}P\{^1H\}$ NMR ($CDCl_3$, 121.66 MHz, 298 K) [$(Mes_3P)_2Au$][$Au(^{13}CN)_2$]: δ 6.33 (br). [(Mes_3P)Au(^{13}CN)]: δ 5.32 (d, $^2J_{C,P}$ = 121 Hz).

*[(SIDipp)Au(CN^tBu)][SbF_6] ([**6**][SbF_6]).* A mixture of (SIDipp)AuCl (0.113 g, 0.181 mmol) and $AgSbF_6$ (0.062 g, 0.181 mmol) in dichloromethane (ca. 8 mL) was stirred for 30 min at room temperature to obtain an off-white precipitate. The resulting mixture was filtered through a pad of Celite via canula, and the filtrate was concentrated to ∼3 mL under reduced pressure. The mixture was cooled to −18 °C (using ice/acetone bath), and ^{t}BuNC (0.018 g, 0.217 mmol) was added. The reaction mixture was stirred for 1 h, and the solution was kept in a refrigerator at 0 °C to obtain colorless prism shaped crystals of [(SIDipp)Au(CN^tBu)][SbF_6] (0.093 g, 57% yield). ^1H NMR ($CDCl_3$, 500.16 MHz, 298 K): δ 7.48 (t, 2H, $^3J_{HH}$ = 8 Hz, C_6H_3), 7.28 (d, 4H, $^3J_{HH}$ = 8 Hz, C_6H_3), 4.24 (s, 4H, CH_2), 3.03 (sept, 4H, $^3J_{HH}$ = 6.9 Hz, $CH(CH_3)_2$), 1.47 (s, 9H, $C(CH_3)_3$), 1.37 (d, 12H, $^3J_{HH}$ = 6.9 Hz, $CH(CH_3)_2$), 1.33 (d, 12H, $^3J_{HH}$ = 6.9 Hz, $CH(CH_3)_2$). $^{13}C\{^1H\}$ NMR ($CDCl_3$, 125.77 MHz, 298 K): δ 199.9 (Au−NCN), 147.0, 133.1, 130.6, 125.0, 54.5, 29.8, 29.0, 25.6, 24.1; CN and C^{t}Bu not detected. IR (KBr, selected bands) cm^{-1}: 2244 (CN). IR (Nujol mull, selected bands) cm^{-1}: 2243 (CN). Anal. Calcd for $C_{32}H_{47}N_3F_6AuSb{\cdot}CH_2Cl_2$: C, 39.98; H, 4.98; N, 4.24. Found: C, 40.32; H, 5.02; N, 4.99%.

*[(SIDipp)Au(cyclooctyne)][SbF_6] ([**8**][SbF_6]).* Cyclooctyne (0.029 g, 0.271 mmol) in dichloromethane (8 mL) was placed in Schlenk flask together with several pieces of 4 Å molecular sieve and degassed by the freeze−pump−thaw method. The degassed cyclooctyne−dichloromethane solution was added to the mixture of $AgSbF_6$ (0.062 g, 0.181 mmol) and (SIDipp)AuCl (0.113 g, 0.181 mmol) as solid at 0 °C. The reaction mixture was stirred for 1 h 0 °C. The resulting mixture was filtered through a pad of Celite via canula, and the filtrate was concentrated to ∼4 mL under reduced pressure. The concentrated solution was layered with hexane and kept in refrigerator at −5 °C to obtain colorless prism shaped crystals of [(SIDipp)Au(cyclooctyne)][SbF_6] (0.089 g, 53% yield). ^1H NMR (CD_2Cl_2, 500.16 MHz, 298 K): δ 7.47 (t, 2H, $^3J_{HH}$ = 8 Hz, C_6H_3), 7.29 (d, 4H, $^3J_{HH}$ = 8 Hz, C_6H_3), 4.25 (s, 4H, CH_2), 3.06 (sept, 4H, $^3J_{HH}$ = 6.9 Hz, $CH(CH_3)_2$), 2.02 (m, 4H, C_8H_{12}), 1.76 (m, 4H, C_8H_{12}), 1.51 (m, 4H, C_8H_{12}), 1.37 (d, 12H, $^3J_{HH}$ = 6.9 Hz, $CH(CH_3)_2$), 1.32 (d, 12H, $^3J_{HH}$ = 6.9 Hz, $CH(CH_3)_2$). $^{13}C\{^1H\}$ NMR (CD_2Cl_2, 125.77 MHz, 298 K): δ 202.5 (Au−NCN), 147.3, 133.0, 131.1, 125.3, 97.4 (cyclooctyne), 54.3, 34.1 (cyclooctyne), 29.4, 28.7 (cyclooctyne), 25.5, 24.2, 22.1 (cyclooctyne). Anal. Calcd for $C_{35}H_{50}N_2F_6AuSb{\cdot}0.5CH_2Cl_2$: C, 43.78; H, 5.28; N, 2.88. Found: C, 43.59; H, 5.01; N, 2.77%.

*[(Mes_3P)Au(cyclooctyne)][SbF_6] ([**9**][SbF_6]).* Cyclooctyne (0.028 g, 0.262 mmol) in dichloromethane (6 mL) was placed in a Schlenk flask together with several pieces of 4 Å molecular sieve and degassed by the freeze−pump−thaw method. The degassed cyclooctyne−dichloromethane solution was added to the mixture of (Mes_3P)AuCl (0.109 g, 0.175 mmol) and $AgSbF_6$ (0.060 g, 0.175 mmol) as solid at 0 °C. The

dx.doi.org/10.1021/ic301869v | Inorg. Chem. 2013, 52, 729−742

reaction mixture was stirred for 3 h and filtered through a pad of Celite via canula. The filtrate was concentrated to ~2 mL, diluted with hexane (2 mL), and cooled at −5 °C for 24 h in a refrigerator to form [(Mes_3P)Au(cyclooctyne)][SbF_6] as a colorless solid (0.105 g, 64% yield). X-ray quality crystals were obtained from dichloromethane solution layered with hexane at −5 °C. *[(Mes_3P)Au(cyclooctyne)][SbF_6] slowly decomposes in CD_2Cl_2 solution at room temperature presumably forming [(Mes_3P)$_2$Au][SbF_6] as one of the products (based on comparison of spectroscopic data to previously reported [(Mes_3P)$_2$Au][BF_4]).*[51] ^{1}H NMR (CD_2Cl_2, 500.16 MHz, 298 K): δ 7.01 (br. s, 3H, C_6H_2), 6.88 (s, 3H, C_6H_2), 2.66 (m, 4H, C_8H_{12}), 2.33 (br, 9H, *o*-CH_3), 2.27 (br, 9H, *p*-CH_3), 2.01 (m, 4H, C_8H_{12}), 1.81 (br s, 9H, *o*-CH_3), 1.72 (m, 4H, C_8H_{12}). ^{13}C{^{1}H} NMR (CD_2Cl_2, 125.77 MHz, 298 K): (selected peaks, cyclooctyne) δ 101.9 (br), 33.9, 29.1, 23.1. ^{31}P{^{1}H} NMR (CD_2Cl_2, 202.47 MHz, 298 K): δ 6.39 (s). Anal. Calcd for $C_{35}H_{45}F_6PAuSb$: C, 45.23; H, 4.88. Found: C, 46.04; H, 4.24%.

X-ray Crystallographic Data. A suitable crystal covered with a layer of paratone-N oil was selected and mounted within a cryo-loop and immediately placed in the low-temperature nitrogen stream. Diffraction data were collected at T = 100(2) K. The data sets were collected on a Bruker SMART APEX CCD diffractometer with graphite monochromated Mo Kα radiation (λ = 0.710 73 Å). The cell parameters were obtained from a least-squares refinement of the spots (from 60 collected frames) using the SMART program. Intensity data were processed using the Saint Plus program. All the calculations for the structure determination were carried out using the SHELXTL package (version 6.14).[68] Initial atomic positions were located by direct methods using XS, and the structures of the compounds were refined by the least-squares method using XL. Absorption corrections were applied by using SADABS. Hydrogen positions were input and refined in a riding manner along with the attached carbons. Crystallographic data are summarized in Table 8.

[(SIDipp)Au(CN)]. This compound crystallized in space group *Pbcm*. All the non-hydrogen atoms were refined with anisotropic displacement parameters. All the hydrogen atoms were placed in ideal positions and refined as riding atoms with relative isotropic displacement parameters. FVAR commands were used to treat occupancy disorder for dichloromethane.

[(Mes_3P)$_2$Au][Au(CN)$_2$]. This compound crystallized in space group $P2_1/n$ with two half complexes appearing in the asymmetric unit. There is a center of inversion at the gold center of [(Mes_3P)$_2$Au] moieties. All the non-hydrogen atoms were refined with anisotropic displacement parameters. All the hydrogen atoms were placed in ideal positions and refined as riding atoms with relative isotropic displacement parameters. ISOR restraints were required to treat Non-Positive Definite messages for Cl atoms from dichloromethane solvent.

[(SIDipp)Au(CN^{t}Bu)][SbF_6]. This compound crystallized in space group $P\bar{1}$ with two independent [(SIDipp)Au(CN^{t}Bu)][SbF_6] moieties in the asymmetric unit. All the non-hydrogen atoms were refined with anisotropic displacement parameters. All the hydrogen atoms were placed in ideal positions and refined as riding atoms with relative isotropic displacement parameters. ISOR restraints were required to treat Non-Positive Definite messages for Cl atoms from dichloromethane solvent.

[(SIDipp)Au(cyclooctyne)][SbF_6]. This compound crystallized in space group $P2_1/c$. All the non-hydrogen atoms were refined with anisotropic displacement parameters. All the hydrogen atoms were placed in ideal positions and refined as riding atoms with relative isotropic displacement parameters. FVAR commands were used to treat occupancy disorder for the cyclooctyne ligand (atoms C32 and C33).

[(Mes_3P)Au(cyclooctyne)][SbF_6]. This compound crystallized in space group $P\bar{1}$ with two independent [(Mes_3P)Au(cyclooctyne)]-[SbF_6] moieties in the asymmetric unit. All the non-hydrogen atoms were refined with anisotropic displacement parameters. All the hydrogen atoms were placed in ideal positions and refined as riding atoms with relative isotropic displacement parameters. The [SbF_6]$^-$ counterion and dichloromethane solvent were disordered and were treated with a combination of FVAR and ISOR restraints. ISOR was used for atoms Cl2, F8, F9, F10, F11, and F12.

COMPUTATIONAL METHODS

Geometry optimizations of the molecules have been carried out without symmetry constraints using Turbomole 6.3.1[69] at the BP86,[69,70]/def2-TZVPP[72] level of theory (denoted BP86/TZVPP). The nature of the stationary points on the potential energy surface has been confirmed as energy minima by frequency calculations. Partial charges (NBO)[73] were calculated at the same level of theory using the Gaussian09 program.[74]

The energy decomposition analysis (EDA) has been carried out with the program package ADF 2009.01[75] at BP86 in conjunction with a triple-ζ-quality basis set using uncontracted Slater-type orbitals (STOs) augmented by two sets of polarization function with a frozen-core approximation for the core electrons using the BP86/TZVPP optimized geometries.[76] This level of theory is denoted as BP86/TZ2P +//BP86/TZVPP. An auxiliary set of s, p, d, f, and g STOs were used to fit the molecular densities and to represent the Coulomb and exchange potentials accurately in each SCF cycle.[77] Scalar relativistic effects were incorporated by applying the zeroth-order regular approximation (ZORA).[78−80]

The energy decomposition analysis (EDA) gives a quantitative description of the chemical bonds in molecules.[81−83] In the EDA developed independently by Morokuma,[84] and Zieglar and Rauk,[85] and the recently introduced EDA-NOCV,[86,87] the bond dissociation energy, D_e, of a molecule AB is divided into the instantaneous interaction energy ΔE_{int} and the preparation energy ΔE_{prep}:

$$\Delta E\,(=-D_e) = \Delta E_{int} + \Delta E_{prep} \tag{1}$$

The preparation energy ΔE_{prep} is the energy which is required to promote the fragments A and B from their equilibrium geometries in the electronic ground state to the geometries and electronic reference state which they have in the molecule. The interaction energy ΔE_{int} can be further divided into three main components

$$\Delta E_{int} = \Delta E_{elstat} + \Delta E_{Pauli} + \Delta E_{orb} \tag{2}$$

where ΔE_{elstat} is the quasiclassical electrostatic interaction energy between the fragments, calculated by means of the frozen electron density distribution of the fragments in the geometry of the molecules. ΔE_{Pauli} refers to the repulsive interactions between the fragments, which are caused by the fact that two electrons with the same spin cannot occupy the same region in space, and can be calculated by enforcing the Kohn−Sham determinant on the superimposed fragments to obey the Pauli principle by antisymmetrization and renormalization. The stabilizing orbital interaction term ΔE_{orb} is calculated in the final step of the energy partitioning analysis when the Kohn−Sham orbitals relax to their optimal form.

The EDA-NOCV[87] method combines charge (NOCV) and energy (EDA) partitioning schemes to decompose the deformation density which is associated with the bond formation, $\Delta\rho$, into different components of the chemical bond. The EDA-NOCV calculations provide pair wise energy contributions for each pair or interacting orbitals to the total bond energy. NOCV (natural orbital for chemical valence)[86,88] is defined as the eigenvector of the valence operator,$\hat{V}$, given by eq 3:

$$\hat{V}\psi_i = \upsilon_i\psi_i \tag{3}$$

In the EDA-NOCV scheme the orbital interaction term, ΔE_{orb}, is given by eq 4

$$\Delta E_{orb} = \sum_{k=1}^{N/2} \Delta E_k^{orb} = \sum_{k=1}^{N/2} \upsilon_k[-F_{-k,-k}^{TS} + F_{k,k}^{TS}] \tag{4}$$

in which $F_{-k,-k}^{TS}$ and $F_{k,k}^{TS}$ are diagonal transition-state Kohn−Sham matrix elements corresponding to NOCVs with the eigenvalues $-\upsilon_k$ and υ_k, respectively. The ΔE_k^{orb} terms of a particular type of bond are assigned by visual inspection of the shape of the deformation density, $\Delta\rho_k$. The EDA-NOCV scheme thus provides information about the

dx.doi.org/10.1021/ic301869v | Inorg. Chem. 2013, 52, 729−742

strength of orbital interactions in terms of both charge ($\Delta\rho_{orb}$) and energy contributions (ΔE_{orb}) in chemical bonds, even in molecules with C_1 symmetry.

■ ASSOCIATED CONTENT

Supporting Information

X-ray crystallographic data (CIF) for (SIDipp)Au(CN), $[(Mes_3P)_2Au][Au(CN)_2]$, $[(SIDipp)Au(CN^tBu)][SbF_6]$, $[(SIDipp)Au(cyclooctyne)][SbF_6]$, and $[(Mes_3P)Au(cyclooctyne)][SbF_6]$, and additional computational study data. This material is available free of charge via the Internet at http://pubs.acs.org.

■ AUTHOR INFORMATION

Corresponding Author

*E-mail: frenking@chemie.uni-marburg.de (G.F.), dias@uta.edu (H.V.R.D.).

Notes

The authors declare no competing financial interest.

■ ACKNOWLEDGMENTS

This work was supported by the National Science Foundation (CHE-0845321) and the Robert A. Welch Foundation (Grant Y-1289). The NSF (CHE-0840509) is thanked for providing funds to upgrade the NMR spectrometer used in this work. The X-ray crystallography was performed in the Center for Nanostructured Materials (CNM) at the University of Texas at Arlington.

■ REFERENCES

(1) Corma, A.; Leyva-Perez, A.; Sabater, M. J. *Chem. Rev.* **2011**, *111*, 1657−1712.
(2) Hashmi, A. S. K. *Angew. Chem., Int. Ed.* **2010**, *49*, 5232−5241.
(3) Hashmi, A. S. K.; Rudolph, M. *Chem. Soc. Rev.* **2008**, *37*, 1766−1775.
(4) Li, Z.; Brouwer, C.; He, C. *Chem. Rev.* **2008**, *108*, 3239−3265.
(5) Schmidbaur, H.; Schier, A. *Organometallics* **2010**, *29*, 2−23.
(6) Hashmi, A. S. K.; Buehrle, M. *Aldrichimica Acta* **2010**, *43*, 27−33.
(7) Min, B. K.; Friend, C. M. *Chem. Rev.* **2007**, *107*, 2709−2724.
(8) Dash, C.; Shaikh, M. M.; Butcher, R. J.; Ghosh, P. *Inorg. Chem.* **2010**, *49*, 4972−4983 and references therein.
(9) Nolan, S. P. *Acc. Chem. Res.* **2011**, *44*, 91−100.
(10) Marion, N.; Nolan, S. P. *Chem. Soc. Rev.* **2008**, *37*, 1776−1782.
(11) Tiekink, E. R. T.; Kang, J.-G. *Coord. Chem. Rev.* **2009**, *253*, 1627−1648.
(12) Widenhoefer, R. A. *Chem.—Eur. J.* **2008**, *14*, 5382−5391.
(13) Hashmi, A. S. K.; Lothschütz, C.; Graf, K.; Häffner, T.; Schuster, A.; Rominger, F. *Adv. Synth. Catal.* **2011**, *353*, 1407−1412.
(14) Hashmi, A. S. K.; Lothschütz, C.; Böhling, C.; Hengst, T.; Hubbert, C.; Rominger, F. *Adv. Synth. Catal.* **2010**, *352*, 3001−3012.
(15) Hashmi, A. S. K.; Hengst, T.; Lothschuetz, C.; Rominger, F. *Adv. Synth. Catal.* **2010**, *352*, 1315−1337.
(16) Dias, H. V. R.; Lovely, C. J. *Chem. Rev.* **2008**, *108*, 3223−3238.
(17) Dias, H. V. R.; Flores, J. A.; Wu, J.; Kroll, P. *J. Am. Chem. Soc.* **2009**, *131*, 11249−11255.
(18) Wu, J.; Kroll, P.; Dias, H. V. R. *Inorg. Chem.* **2009**, *48*, 423−425.
(19) Dias, H. V. R. *Pure Appl. Chem.* **2010**, *82*, 649−656.
(20) Dash, C.; Kroll, P.; Yousufuddin, M.; Dias, H. V. R. *Chem. Commun.* **2011**, *47*, 4478−4480.
(21) Dias, H. V. R.; Dash, C.; Yousufuddin, M.; Celik, M. A.; Frenking, G. *Inorg. Chem.* **2011**, *50*, 4253−4255.
(22) Jones, P. G. *Z. Naturforsch.* **1982**, *37*, 823−824.
(23) Dias, H. V. R.; Jin, W. *Inorg. Chem.* **1996**, *35*, 3687−3694.
(24) Kuster, R.; Seppelt, K. *Z. Anorg. Allg. Chem.* **2000**, *626*, 236−240.
(25) Xu, Q.; Imamura, Y.; Fujiwara, M.; Souma, Y. *J. Org. Chem.* **1997**, *62*, 1594−1598.
(26) Davis, R. J. *Science* **2003**, *301*, 926−927.
(27) Zhu, B.; Angelici, R. J. *J. Am. Chem. Soc.* **2006**, *128*, 14460−14461.
(28) Ye, L.; Wang, Y.; Aue, D. H.; Zhang, L. *J. Am. Chem. Soc.* **2012**, *134*, 31−34.
(29) Hashmi, A. S. K.; Braun, I.; Rudolph, M.; Rominger, F. *Organometallics* **2012**, *31*, 644−661.
(30) Hashmi, A. S. K.; Wieteck, M.; Braun, I.; Nösel, P.; Jongbloed, L.; Rudolph, M.; Rominger, F. *Adv. Synth. Catal.* **2012**, *354*, 555−562.
(31) Hashmi, A. S. K.; Braun, I.; Nösel, P.; Schädlich, J.; Wieteck, M.; Rudolph, M.; Rominger, F. *Angew. Chem., Int. Ed.* **2012**, *51*, 4456−4460.
(32) Lupinetti, A. J.; Frenking, G.; Strauss, S. H. *Angew. Chem., Int. Ed.* **1998**, *37*, 2113−2116.
(33) Lupinetti, A. J.; Strauss, S. H.; Frenking, G. *Progress in Inorganic Chemistry*; Karlin, K. D., Ed.; Wiley: New York, 2001; Vol. *49*, p 1.
(34) Martinez-Salvador, S.; Fornies, J.; Martin, A.; Menjon, B. *Angew. Chem., Int. Ed.* **2011**, *50*, 6571−6574.
(35) Aubke, F.; Wang, C. *Coord. Chem. Rev.* **1994**, *137*, 483−524.
(36) Liang, B.; Andrews, L. *J. Phys. Chem. A* **2000**, *104*, 9156−9164.
(37) Dell'Amico, D. B.; Calderazzo, F. *Gold Bull.* **1997**, *30*, 21−24.
(38) Schmidbaur, H.; Schier, A. *Chem. Soc. Rev.* **2012**, *41*, 370−412.
(39) Veldkamp, A.; Frenking, G. *Organometallics* **1993**, *12*, 4613−4622.
(40) Antes, I.; Dapprich, S.; Frenking, G.; Schwerdtfeger, P. *Inorg. Chem.* **1996**, *35*, 2089−2096.
(41) Diedenhofen, M.; Wagener, T.; Frenking, G. In *Computational Organometallic Chemistry*; Cundari, T., Ed.; Marcel Dekker: New York, 2001; p 69.
(42) Diefenbach, A.; Bickelhaupt, F. M.; Frenking, G. *J. Am. Chem. Soc.* **2000**, *122*, 6449−6458.
(43) Lupinetti, A.; Fau, S.; Frenking, G.; Strauss, S. H. *J. Phys. Chem. A* **1997**, *101*, 9551−9559.
(44) Lupinetti, A. J.; Jonas, V.; Thiel, W.; Strauss, S. H.; Frenking, G. *Chem.—Eur. J.* **1999**, *5*, 2573−2583.
(45) Frenking, G.; Loschen, C.; Krapp, A.; Fau, S.; Strauss, S. H. *J. Comput. Chem.* **2007**, *28*, 117−126.
(46) Baker, M. V.; Barnard, P. J.; Brayshaw, S. K.; Hickey, J. L.; Skelton, B. W.; White, A. H. *Dalton Trans.* **2005**, 37−43.
(47) Gaillard, S.; Slawin, A. M. Z.; Nolan, S. P. *Chem. Commun.* **2010**, *46*, 2742−2744.
(48) De, F. P.; Scott, N. M.; Stevens, E. D.; Nolan, S. P. *Organometallics* **2005**, *24*, 2411−2418.
(49) Jones, P. G.; Lautner, J. *Acta Crystallogr.* **1988**, *C44*, 2091−2093.
(50) Hormann, A. L.; Shaw, C. F.; Bennett, D. W.; Reiff, W. M. *Inorg. Chem.* **1986**, *25*, 3953−3957.
(51) Bayler, A.; Bowmaker, G. A.; Schmidbaur, H. *Inorg. Chem.* **1996**, *35*, 5959−5960.
(52) Isab, A. A.; Hussain, M. S.; Akhtar, M. N.; Wazeer, M. I. M.; Al-Arfaj, A. R. *Polyhedron* **1999**, *18*, 1401−1409.
(53) Bayler, A.; Schier, A.; Bowmaker, G. A.; Schmidbaur, H. *J. Am. Chem. Soc.* **1996**, *118*, 7006−7007.
(54) Assefa, Z.; Omary, M. A.; McBurnett, B. G.; Mohamed, A. A.; Patterson, H. H.; Staples, R. J.; Fackler, J. P. *Inorg. Chem.* **2002**, *41*, 6274−6280.
(55) Ehlers, A. W.; Dapprich, S.; Vyboishchikov, S. F.; Frenking, G. *Organometallics* **1996**, *15*, 105−117.
(56) Dietz, O.; Rayon, V. M.; Frenking, G. *Inorg. Chem.* **2003**, *42*, 4977−4984.
(57) Loschen, C.; Frenking, G. *Inorg. Chem.* **2004**, *43*, 778−784.
(58) Das, A.; Dash, C.; Yousufuddin, M.; Celik, M. A.; Frenking, G.; Dias, H. V. R. *Angew. Chem., Int. Ed.* **2012**, *51*, 3940−3943.
(59) Brown, T. J.; Widenhoefer, R. A. *Organometallics* **2011**, *30*, 6003−6009.
(60) Hooper, T. N.; Green, M.; Russell, C. A. *Chem. Commun.* **2010**, *46*, 2313−2315.

(61) Salvi, N.; Belpassi, L.; Tarantelli, F. *Chem.—Eur. J.* **2010**, *16*, 7231−7240.
(62) Zuccaccia, D.; Belpassi, L.; Rocchigiani, L.; Tarantelli, F.; Macchioni, A. *Inorg. Chem.* **2010**, *49*, 3080−3082.
(63) Fluegge, S.; Anoop, A.; Goddard, R.; Thiel, W.; Fuerstner, A. *Chem.—Eur. J.* **2009**, *15*, 8558−8565.
(64) Alyea, E. C.; Ferguson, G.; Gallagher, J. F.; Malito, J. *Acta Crystallogr., Sect. C* **1993**, *C49*, 1473−6.
(65) (a) Wilson, D. J. D.; Couchman, S. A.; Dutton, J. L. *Inorg. Chem.* **2012**, *51*, 7657−7668. (b) Sato, T.; Hirose, Y.; Yoshioka, D.; Oi, S. *Organometallics* **2012**, *31*, 6995−7003.
(66) Brandsma, L.; Verkruijsse, H. D. *Synthesis* **1978**, 290.
(67) Bott, R. C.; Bowmaker, G. A.; Buckley, R. W.; Healy, P. C.; Perera, M. C. S. *Aust. J. Chem.* **2000**, *53*, 175−181.
(68) Sheldrick, G. M. *SHELXTL, Version 6.14*; Bruker Analytical X-ray Systems, Inc.: Madison, WI, 2000.
(69) Ahlrichs, R.; Baer, M.; Haeser, M.; Horn, H.; Koelmel, C. *Chem. Phys. Lett.* **1989**, *162*, 165−169.
(70) Becke, A. D. *Phys. Rev. A: Gen. Phys* **1988**, *38*, 3098−3100.
(71) Perdew, J. P. *Phys. Rev. B* **1986**, *33*, 8822−8824.
(72) Weigend, F.; Ahlrichs, R. *Phys. Chem. Chem. Phys.* **2005**, *7*, 3297−3305.
(73) Reed, A. E.; Weinstock, R. B.; Weinhold, F. *J. Chem. Phys.* **1985**, *83*, 735−746.
(74) Frisch, M. J.; Trucks, G. W.; Schlegel, H. B.; Scuseria, G. E.; Robb, M. A.; Cheeseman, J. R.; Scalmani, G.; Barone, V.; Mennucci, B.; Petersson, G. A.; Nakatsuji, H.; Caricato, M.; Li, X.; Hratchian, H. P.; Izmaylov, A. F.; Bloino, J.; Zheng, G.; Sonnenberg, J. L.; Hada, M.; Ehara, M.; Toyota, K.; Fukuda, R.; Hasegawa, J.; Ishida, M.; Nakajima, T.; Honda, Y.; Kitao, O.; Nakai, H.; Vreven, T.; Montgomery, J. A., Jr.; Peralta, P. E.; Ogliaro, F.; Bearpark, M.; Heyd, J. J.; Brothers, E.; Kudin, K. N.; Staroverov, V. N.; Kobayashi, R.; Normand, J.; Raghavachari, K.; Rendell, A.; Burant, J. C.; Iyengar, S. S.; Tomasi, J.; Cossi, M.; Rega, N.; Millam, N. J.; Klene, M.; Knox, J. E.; Cross, J. B.; Bakken, V.; Adamo, C.; Jaramillo, J.; Gomperts, R.; Stratmann, R. E.; Yazyev, O.; Austin, A. J.; Cammi, R.; Pomelli, C.; Ochterski, J. W.; Martin, R. L.; Morokuma, K.; Zakrzewski, V. G.; Voth, G. A.; Salvador, P.; Dannenberg, J. J.; Dapprich, S.; Daniels, A. D.; Farkas, Ö.; Ortiz, J. V.; Cioslowski, J.; Fox, D. J. *Gaussian 09*, Revision C.01 ; Gaussian, Inc.: Wallingford, CT, 2010.
(75) Te, V. G.; Bickelhaupt, F. M.; Baerends, E. J.; Fonseca, G. C.; Van, G. S. J. A.; Snijders, J. G.; Ziegler, T. *J. Comput. Chem.* **2001**, *22*, 931−967.
(76) Snijders, J. G.; Baerends, E. J.; Vernoojs, P. *At. Data. Nucl. Data Tables* **1982**, *26*, 483.
(77) Krijn, J.; Baerends, E. J. *Fit Functions in the HFS-Method, Internal Report (in Dutch)*; Vrije Universiteit, 1984.
(78) van Lenthe, E.; Baerends, E. J.; Snijders, J. G. *J. Chem. Phys.* **1993**, *99*, 4597−4610.
(79) van Lenthe, E.; Baerends, E. J.; Snijders, J. G. *J. Chem. Phys.* **1994**, *101*, 9783−9792.
(80) van Lenthe, E.; Ehlers, A.; Baerends, E.-J. *J. Chem. Phys.* **1999**, *110*, 8943−8953.
(81) von Hopffgarten, M.; Frenking, G. *Wiley Interdiscip. Rev.: Comput. Mol. Sci.* **2012**, *2*, 43−62.
(82) Lein, M.; Frenking, G. In *Theory and Applications of Computational Chemistry*; Clliford, E. D., Gernot, F., Kwang, S. K., Gustavo, E. S., Eds.; Elsevier: Amsterdam, 2005; pp 291−372.
(83) Frenking, G.; Wichmann, K.; Frohlich, N.; Loschen, C.; Lein, M.; Frunzke, J.; Rayon, V. M. *Coord. Chem. Rev.* **2003**, *238*−*239*, 55−82.
(84) Morokuma, K. *J. Chem. Phys.* **1971**, *55*, 1236−1244.
(85) Ziegler, T.; Rauk, A. *Inorg. Chem.* **1979**, *18*, 1558−1565.
(86) Mitoraj, M.; Michalak, A. *Organometallics* **2007**, *26*, 6576−6580.
(87) Mitoraj, M. P.; Michalak, A.; Ziegler, T. *J. Chem. Theory Comput.* **2009**, *5*, 962−975.
(88) Michalak, A.; Mitoraj, M.; Ziegler, T. *J. Phys. Chem. A* **2008**, *112*, 1933−1939.
(89) Dellamico, D. B.; Calderazzo, F.; Robino, P.; Segre, A. *J. Chem. Soc., Dalton Trans.* **1991**, 3017−3020.
(90) Calderazzo, F. *J. Organomet. Chem.* **1990**, *400*, 303−320.
(91) Willner, H.; Aubke, F. *Inorg. Chem.* **1990**, *29*, 2195−2200.
(92) Willner, H.; Schaebs, J.; Hwang, G.; Mistry, F.; Jones, R.; Trotter, J.; Aubke, F. *J. Am. Chem. Soc.* **1992**, *114*, 8972−8980.
(93) Hurlburt, P. K.; Rack, J. J.; Luck, J. S.; Dec, S. F.; Webb, J. D.; Anderson, O. P.; Strauss, S. H. *J. Am. Chem. Soc.* **1994**, *116*, 10003−10014.
(94) Adelhelm, M.; Bacher, W.; Hohn, E. G.; Jacob, E. *Chem. Ber.* **1991**, *124*, 1559−1561.
(95) Shi, C. C.; Chen, C. S.; Hsu, S. C. N.; Yeh, W. Y.; Chiang, M. Y.; Kuo, T. S. *Inorg. Chem. Commun.* **2008**, *11*, 1264−1266.
(96) Al-Arfaj, A. R.; Reibenspies, J. H.; Hussain, M. S.; Darensbourg, M. Y.; Akhtar, N.; Isab, A. A. *Acta Crystallogr.* **1997**, *C53*, 1553−1555.
(97) Al-Arfaj, A. R.; Reibenspies, J. H.; Hussain, M. S.; Isab, A. A. *Acta Crystallogr.* **1998**, *C54*, 716−719.
(98) Hussain, M. S.; Al-Arfaj, A. R.; Akhtar, M. N.; Isab, A. A. *Polyhedron* **1996**, *15*, 2781−2785.
(99) Yano, T.; Wasada-Tsutsui, Y.; Arii, H.; Yamaguchi, S.; Funahashi, Y.; Ozawa, T.; Masuda, H. *Inorg. Chem.* **2007**, *46*, 10345−10353.
(100) Eggleston, D. S.; Chodosh, D. F.; Webb, R. L.; Davis, L. L. *Acta Crystallogr.* **1986**, *C42*, 36−38.
(101) Elbjeirami, O.; Omary, M. A.; Stender, M.; Balch, A. L. *Dalton Trans.* **2004**, 3173−3175.
(102) Schneider, W.; Angermaier, K.; Sladek, A.; Schmidbaur, H. *Z. Naturforsch.* **1996**, *51*, 790−800.
(103) Che, C. M.; Yip, H. K.; Wong, W. T.; Lai, T. F. *Inorg. Chim. Acta* **1992**, *197*, 177−183.
(104) Mathieson, T. J.; Langdon, A. G.; Milestone, N. B.; Nicholson, B. K. *Chem. Commun.* **1998**, 371−372.
(105) Rombke, P.; Schier, A.; Wiesbrock, F.; Schmidbaur, H. *Inorg. Chim. Acta* **2003**, *347*, 123−128.
(106) Vicente, J.; Chicote, M. T.; Abrisqueta, M. D.; Guerrero, R.; Jones, P. G. *Angew. Chem., Int. Ed.* **1997**, *36*, 1203−1205.
(107) Canovese, L.; Visentin, F.; Levi, C.; Bertolasi, V. *Organometallics* **2011**, *30*, 875−883.